MiR-30e-3p influences tumor phenotype through MDM2/TP53 axis and predicts sorafenib resistance in hepatocellular carcinoma

MiR-30e-3p influences tumor phenotype through *MDM2*/*TP53* axis and predicts sorafenib resistance in hepatocellular carcinoma

Laura Gramantieri[1$], Daniela Pollutri[1,2], Martina Gagliardi[1,3], Catia Giovannini[1,3], Santina Quarta[4], Manuela Ferracin[2], Andrea Casadei-Gardini[5], Elisa Callegari[6], Sabrina De Carolis[1,2], Sara Marinelli[1,3], Francesca Benevento[3], Francesco Vasuri[7], Matteo Ravaioli[8], Matteo Cescon[3,8], Fabio Piscaglia[3], Massimo Negrini[6], Luigi Bolondi[1,3], Francesca Fornari[1,3,$]

[1] Center for Applied Biomedical Research, St.Orsola-Malpighi University Hospital, Bologna, Italy

[2] Department of Experimental, Diagnostic and Specialty Medicine, University of Bologna, Italy

[3] Department of Medical and Surgical Sciences, University of Bologna, Bologna, Italy

[4] Department of Medicine, University of Padua, Padua, Italy

[5] Department of Oncology and Hematology, Division of Oncology, University of Modena and Reggio Emilia, Italy

[6] Department of Morphology, Surgery and Experimental Medicine, University of Ferrara, Italy

[7] Pathology Unit, St.Orsola-Malpighi University Hospital, Bologna, Italy

[8] General Surgery and Transplant Unit, St.Orsola-Malpighi University Hospital, Bologna, Italy

[$]Corresponding Authors

Running title: MiR-30e predicts sorafenib escape in HCC

Key words: HCC, microRNA, miR-30e, Sorafenib

Corresponding Authors:
Francesca Fornari, Laura Gramantieri
Address: Via Massarenti, 9, 40138, Bologna, Italy.
Tel/Fax: +390512143902
E-mail: francesca.fornari2@unibo.it, laura.gramantieri@aosp.bo.it

Conflict of interest: The Authors have no conflict of interest to declare

Abstract

The molecular background of hepatocellular carcinoma (HCC) is highly heterogeneous and biomarkers predicting response to treatments are an unmet clinical need. We investigated miR-30e-3p contribution to HCC phenotype and response to sorafenib, as well as the mutual modulation of *TP53/MDM2* pathway, in HCC tissues and preclinical models. MiR-30e-3p was downregulated in human and rat HCCs and its downregulation associated with *TP53* mutations. *TP53* contributed to miR-30e-3p biogenesis and *MDM2* was identified among its target genes, establishing a miR-30e-3p/*TP53*/*MDM2* feedforward loop and accounting for miR-30e-3p dual role based on *TP53* status.

EpCAM, PTEN and p27 were demonstrated as miR-30e-3p additional targets mediating its contribution to stemness and malignant features. In a preliminary cohort of HCC patients treated with sorafenib, increased miR-30e-3p circulating levels predicted the development of resistance.

In conclusion, molecular background dictates miR-30e-3p dual behavior in HCC. Mdm2 targeting/p53 axis plays a predominant tumor-suppressor function in wild type *TP53* contexts, whereas other targets such as PTEN, p27 and EpCAM gain relevance and mediate miR-30e-3p oncogenic role in non-functional *TP53* backgrounds. Increased circulating levels of miR-30e-3p predict the development of sorafenib resistance in a preliminary series of HCC patients and deserve future investigations.

Statement of significance

The dual role of miR-30e-3p in hepatocellular carcinoma clarifies how the molecular context dictates the tumor suppressor or oncogenic function played by microRNAs.

Introduction

Hepatocellular carcinoma (HCC) accounts for 90% of primary liver cancers representing the second leading cause of cancer mortality with increasing incidence in western countries [1]. HCC is characterized by a high inter- and intra-individual tumor heterogeneity: the former ascribed to different risk factors and genomic contexts [2] and the latter to clonal evolution of cancer cells [3], both contributing to limited targeted therapy efficacy. Primary resistance and escape from antitumor strategies remain poorly understood and no biomarker predicting response to sorafenib or other targeted treatments has been identified so far, highlighting the need for novel tools to allocate patients to the best treatment.

The deregulation of tumor-specific microRNAs (miRNAs) with tumor suppressor or oncogenic properties has been described [4, 5]. Our group and others demonstrated the key role of deregulated miRNAs in tumor progression and metastasis [6, 7], as well as their involvement in drug resistance phenotype [8-10]. Aberrant expression of miR-30 family members is a frequent event in solid tumors [11, 12] displaying a prominent connection with other deregulated miRNAs in neoplastic tissues [13]. The miR-30 family contains five members encoded by six genes located on three distinct loci of the human genome (chromosomes 1, 6 and 8) giving rise to six mature miRNAs (miR-30a, -30b, -30c-1, -30c-2, -30d, -30e) with the same seed sequence. The downregulation of these miRNAs was associated with proliferation and invasion, as well as with induction of epithelial-to-mesenchymal transition (EMT), exerted by direct targeting of EMT-associated factors [14, 15] and cell adhesion molecules [16]. Remarkably, besides studies supporting the tumor suppressor role of miR-30 family, other studies point to its opposite behavior [17, 18].

TP53 is one of the most frequently mutated gene in human cancers with about 30% of affected HCC cases [19]. *TP53* regulates miRNA expression by acting at two different levels: on one hand, it activates their transcriptional regulation [20-22] and, on the other hand, it interferes with their maturation process by interacting with key molecules, such as Drosha and p68 RNA

helicase [23]. Notably, *TP53* regulates the expression of miR-30 family members contributing to cell invasion and distal spreading as reported in colorectal and breast cancers [24, 25].

Despite the prominent role of miR-30 family as tumor suppressor miRNAs, there are conflicting data regarding its aberrant expression in HCC. Previous studies reported the downregulation of miR-30a and miR-30e and the upregulation of miR-30d [26-28]. Although miR-30 was reported as participating in hepatobiliary development [29], its functional roles in HCC remain poorly understood. Here, we investigated the expression of miR-30 family members in two HCC patient cohorts, in a HCC animal model and in HCC cells, and focused on miR-30e-3p, characterizing its biological activity as well as its involvement in drug resistance and modulation of *MDM2*/*TP53* and *PTEN/AKT* axes. Moreover, we investigated circulating miR-30e-3p levels in a preliminary series of HCC patients and in preclinical models in order to evaluate its contribution as a non-invasive biomarker of treatment response.

Materials and Methods

HCC study cohorts

HCC and cirrhotic tissues were obtained from two independent cohorts of patients undergoing liver surgery for HCC at the Department of Surgery and Transplant Unit of St. Orsola-Malpighi University Hospital of Bologna. The discovery cohort consists of 22 patients, whereas the validation cohort consists of 48 patients, all enrolled at the Department of Surgery of St. Orsola-Malpighi University Hospital. We collected tissue samples at surgery and stored as previously described [30]. Local ethics committee of St. Orsola-Malpighi University Hospital approved this study (138/2015/O/Tess). Normal liver tissues were from patients undergoing liver surgery for traumatic lesions or haemangioma resection. The clinical characteristics of patients are detailed in Supplementary Table S1. *TP53* mutations were identified as previously described [20].

A further cohort of sorafenib-treated advanced HCC patients (Table S2) was tested for serum miR-30e-3p levels before treatment and at two-month follow-up assessment. Sera samples, obtained after the local committee approval (271/2012/O/Oss), were processed as previously described [31]. Informed written consent has been obtained from patients enrolled in this study.

HCC animal models

The diethyl-nitrosamine (DEN)-induced HCC rat model and the xenograft model were established and treated as previously described [9]. Total RNA was extracted from frozen tissues by using TRIzol Reagent (Invitrogen) and was analyzed by microarray and QPCR. Local ethics committee approved the study protocols (14/70/12 and 23/79/14).

Microarray analysis

RNAs from 22 rat samples (12 HCCs, 8 surrounding livers and 2 normal livers) were hybridized on Agilent rat whole-genome miRNAs microarray (#G4471A_046066 Release 19.0, Agilent

Technologies). One-color gene expression was performed according to the manufacturer's procedure. Raw data are available in ArrayExpress repository (accession number E-MTAB-7624).

Technical details are described in Supplementary section.

Cell culture and treatments

HCC cell lines were cultured as previously described [9]. Starvation was obtained culturing cells in media without FBS for 48-60 hours. Cells were treated with 5.0-7.5 μM sorafenib-tosylate (Bayer) or Nutlin-3 (Sigma-Aldrich) or with 1.0-2.0 μg/ml of doxorubicin (Pfizer) for 48 hours. Cell transfection and proliferation, clonogenic and sphere formation assays are detailed in Supplementary Material. Genetics Unit at S.Orsola-Malpighi Hospital performed HCC authentication and cell identification was obtained by online STR analysis (https://www.dsmz.de/).

Reporter assays

3' untranslated regions (3'UTR) of *MDM2*, *CDKN1B/p27*, *PTEN* and *EpCAM* mRNAs were amplified by PCR as reported in Supplementary Table S2. Mutagenesis of miR-30e-3p seed sequence was performed by using QuikChange II Site-Directed Mutagenesis Kit (Agilent Technologies) following manufacturer's instruction (Supplementary Table S3). Sanger sequencing verified mutated sequences. Dual-luciferase reporter and p53 activity assays were performed as previously described [32].

Real-time PCR

TaqMan MicroRNA Assays (Applied Biosystems) were used to evaluate miRNA expression, as previously described [30]. RNU6B was used as housekeeping gene. Quantitative PCR (qPCR)

was used for gene expression analysis. β-actin and GAPDH housekeeping genes were considered for gene normalization. QPCR experiments were run in triplicate. Primers and conditions are detailed in Supplementary Table S4.

Western blot

Western blot (WB) was used to analyze protein extracts (30 µg) from cell and tissues with antibodies reported in Supplementary Table S5. ChemiDocTM XRS+ (Image LabTM Software, Bio-Rad) was employed to quantify digital images of X-ray films. WB analysis was performed in duplicate.

Chromatin immunoprecipitation and electrophoretic mobility shift assay

HepG2 cells were subjected to chromatin immunoprecipitation (ChIP) with a polyclonal p53 antibody (Novocastra) as previously described [21]. Primers and conditions are reported in Supplementary Table S4. Amplicon design has been detailed in Supplementary Material. Electrophoretic mobility shift assay (EMSA) was performed with nuclear extract (NE) from Nutlin-3 treated HepG2 cells by using LightShift Chemiluminescent EMSA Kit (Thermo Scientific) as previously described [21]. Probe sequences are reported in Supplementary Table S6.

Flow cytometry

Annexin-V assay was performed in duplicate by flow cytometry (FACSaria I, BD) as previously reported [33]. Annexin-V assay in miR-30e-3p overexpressing HepG2 cells was assessed on Cytoflex S (Beckam Coulter). Immunophenotype analysis of EpCAM was performed by using CD326 monoclonal antibody (MH99)-Alexa Fluor 488 (eBioscience).

Cell invasion and wound healing assay

Real-time cell invasion, performed on xCELLigence DP instrument (ACEA), and wound healing assays were executed as previously described [34].

Caspase activity assay

Caspase pathway activation was evaluated by Caspase-Glo 3/7 assay (Promega) according to manufacturer's instructions. Each sample was performed in quadruplicate in two independent experiments.

Serum and exosome miRNA extraction

Isolation of circulating miRNAs from exosomes, cell culture supernatant, and serum was executed as previously reported [9, 31].

Statistical analysis

Differences between two or more groups were analyzed using unpaired Student's t-test or ANOVA. Tukey's post hoc test was used for comparisons among groups after ANOVA analysis. Pearson's correlation coefficient was used to investigate relationships between two variables. Time to recurrence (TTR) curve based on miR-30e-3p levels was computed by Kaplan-Meier product-limit method and compared using a log-rank test. Paired t-test was used to evaluate the relationship between circulating miR-30e-3p and response to sorafenib in HCC patients analyzed both before and on treatment. Reported p-values were two-sided and considered significant when lower than 0.05. Statistical calculations were executed using SPSS version 20.0 (SPSS inc). * $p<0.05$, ** $p<0.01$, *** $p<0.001$, **** $p<0.0001$.

Results

MiR-30e-3p is downregulated in HCC and associates with *TP53* status

We previously reported a deregulation of miR-30 family members in histologically aggressive HCCs [35]. Here, we confirmed in a first patient cohort, a decrease of miR-30e-3p in 73% of HCCs in comparison to matched cirrhotic livers (t-test; p=0.0002), showing a mean downregulation of 1.7-fold (**Figure 1A**). Similarly, a decrease of miR-30e-5p and miR-30a-3p was detected in 64% of tumors with an average 1.6-fold change (t-test; p=0.003 and p=0.008, respectively) (**Figure 1B, C**). A positive correlation between these miR-30 family members was detected in HCC and cirrhotic human samples (**Figure S1A-F**), suggesting common regulation mechanisms for these miR-30 family members.

We next tested the DEN-induced HCC rat model [9] by microarray analysis on 12 HCCs and 10 non-cancerous livers. The downregulation of five miRNAs belonging to miR-30 family was observed in tumors compared to surrounding livers (**Figure S2 and Table S7**). In rat HCC, miR-30e-3p decreased in 64% of tumors, showing a 1.5-fold change (t-test; p=0.034), mirroring findings from human HCCs (**Figure 1D**). MiR-30e-5p and miR-30a-3p were downregulated in 59% and 32% of rat HCCs, showing no difference between tumor and non-tumor samples (**Figure 1E, F**). The discrepancy between human and rat HCCs might be ascribed to the lack of cirrhotic microenvironment in the rat model.

In the validation cohort, we confirmed miR-30e-3p, miR-30e-5p and miR-30a-3p downregulation in HCCs with respect to both matched cirrhosis (Tukey's post hoc test; p=0.012, p=0.013 and p=0.025, respectively) and normal livers (Tukey's post hoc test; p=0.046, p=0.001 and p=0.044, respectively) (**Figure 1G-I**). Here, we focused on miR-30e-3p, which is the most downregulated miRNA in human and rat HCCs.

Since *TP53* is mutated in about 30% of HCCs and it establishes complex regulatory networks with miRNAs [1, 36], we investigated the relationship between *TP53* status and miR-30e-3p in

HCC. Lower miR-30e-3p levels were observed in *TP53* mutated HCCs while no difference was found for primary miR-30e (pri-miR-30e) levels (**Figure 1J, K**). Remarkably, a negative correlation between primary and mature miR-30e levels was found in HCCs (Pearson's correlation; R=-0.32) (**Figure S3A**), suggesting a role for post-transcriptional mechanisms in miR-30e biogenesis regulation. Interestingly, after splitting HCCs according to *TP53* status, a negative correlation was confirmed between primary and mature miRNA levels in *TP53* mutated cases, while a trend towards a positive correlation was found in *TP53* WT cases (**Figure S3B, C**). These findings suggest an impairment of miR-30e-3p maturation by mutant p53 isoforms which were previously reported to interfere with the functional assembly of Drosha/p68 processing complex [23].

TP53 influences miR-30e-3p transcription and biogenesis in HCC cells

To start dissecting p53 involvement in miR-30e biogenesis in HCC, we modulated its expression in *TP53* WT HepG2 cells by using different strategies. First, we investigated the influence of p53 silencing on miR-30e primary transcript and mature isoforms. As showed in Figure 2A, a decrease of primary and mature miR-30e-3p and miR-30e-5p levels was detected in p53-silenced cells. MiR-34a was used as a positive control since it represents the first identified p53-target miRNA [37], whereas p53 silencing was verified by WB and qPCR analyses of target genes (**Figure 2A**). Secondly, we investigated the effect of p53 overexpression in HepG2 cells following transfection of a p53-overexpressing vector or treatment with Nutlin-3, a *MDM2* inhibitor. In line, an increase of miR-30e primary transcript and mature miRNA isoforms was detected in both experimental settings (**Figure 2B, C**). Notably, Nutlin-3 administration led to a stronger p53 transcriptional activation with respect to p53-overexpressing vector, as confirmed by the extent of variation of *CDKN1A/p21* and *MDM2* mRNAs. In turn, this resulted in higher pri-miR-30e levels, but not mature isoforms (**Figure 2B, C**), letting us to speculate that

mdm2/p53 axis might have an additional role in miR-30e biogenesis. To investigate p53 involvement in miRNA maturation, we quantified primary and mature miR-30e levels in p53-deleted (CRISPR/Cas9 technology) HepG2 cells and p53-null Hep3B cells following Nutlin-3 treatment. In line with p53 absence, no increase of miR-30e primary transcript was observed, whereas increased mature miRNA isoforms were detected in both treated cell lines (**Figure 2D, E**), confirming p53 role in miRNA processing impairment during Nutlin-3 administration. Since Dicer1 promoter contains several p63/p53 responsive elements [38], we investigated Dicer1 expression in HepG2 cells following p53 overexpression or Nutlin-3 treatment in both p53 WT and p53-deleted cells. A downregulation of Dicer1 was observed in Nutlin-3 treated HepG2 cells, but not in p53-overexpressing cells, which is in line with miRNA maturation impairment detected after Nutlin-3 administration in p53 WT cells (**Figure S3D, E**). On the contrary, higher Dicer1 levels were detected in p53-deleted HepG2 and p53 null Hep3B cells (**Figure S3F, G**), suggesting that mdm2 inhibition by Nutlin-3 influences miR-30e processing by regulating Dicer1 transcription in a p53-dependent and independent manner.

To go deeper into p53-mediated mechanisms regulating miR-30e expression, we overexpressed WT and mutant (truncated, dominant negative) *TP53* isoforms in p53-deleted Hep3B and p53 WT HepG2 cells, respectively. As displayed in Figure 2F, an increase of primary and mature miR-30e isoforms was observed in *TP53*-overexpressing Hep3B cells confirming its role in miRNA transcription. Interestingly, mutant p53 expression in HepG2 cells decreased miR-30e transcription and, consequently, mature isoforms (**Figure 2G**), suggesting a negative role for p53 mutations in miR-30e regulation. These findings demonstrate that *TP53* WT isoform is necessary to induce miR-30e transcription in HCC cells and that p53/mdm2 axis is involved in a multi-step regulation of miR-30e biogenesis.

To prove p53 binding to hypothetical consensus elements in proximity of miR-30e precursor region, a ChIP experiment was conducted in control and Nutlin-3 treated HepG2 cells. Six amplicons containing *TP53* hypothetical binding sites were designed in a DNA region spanning

from –4000 to +1000 nucleotides, considering +1 the first nucleotide of miR-30e precursor (**Figure S3H**). This region was chosen based on described promoter distance for intronic miRNA [39] and due to the presence of histone modifications (**Figure S3I**). The ChIP analysis showed an enrichment of three out of six p53 hypothetical binding sites, namely BS1, BS2 and BS6, in Nutlin-3 treated cells only (**Figure S3J**), demonstrating that p53 activation strengthen its binding to miR-30e-3p genomic region favoring pri-miR-30e regulation. EMSA assay further confirmed p53 binding to hypothetical consensus sites identified in the ChIP experiment, showing a specific shift for BS1, BS2 and BS6 probes in presence of nuclear extracts from Nutlin-3 treated HepG2 cells (**Figure S3K**).

Notably, a positive correlation (Pearson's correlation; R=0.71) exists between pri-miR-30e and its host gene, nuclear transcription factor Y subunit gamma (*NFYC*, NM_014223) in HCCs, whereas a negative correlation (Pearson's correlation; R=-0.76) was found between mature miR-30e-3p and *NFYC*, outlining the relevance of maturation process in the regulation of miR-30e levels (**Figure S3L, M**).

MiR-30e-3p establishes a *TP53* positive feedback loop through *MDM2* targeting

To investigate the interplay between miR-30e-3p and *TP53*, we interrogated bioinformatics tools and identified the principal p53 negative regulator, *MDM2* (NM_002392), as a hypothetic miR-30e-3p target gene containing three complementary binding sites (**Figure 3A**). We quantified miR-30e-3p levels in seven HCC cell lines and compared its expression with mean values observed in HCCs, cirrhosis and normal livers (**Figure 3B**). In order to avoid a confounding effect due *TP53/MDM2* auto-regulatory loop, we performed a functional analysis in HCC cell lines with mutated or null p53 isoform. Huh-7, Hep3B and SNU475 cells were chosen based on their low/intermediate miR-30e-3p basal levels, whereas SNU449 cells were selected because of their high basal levels (**Figure 3B**). MiR-30e-3p overexpression in Huh-7, Hep3B and SNU475

cells decreased mdm2 mRNA and protein levels, whereas miRNA silencing in SNU449 cells increased its mRNA and protein expression (**Figure 3C-F**). Subsequently, we explored *MDM2* targeting by miR-30e-3p in HepG2 cells. We observed increased mRNA and protein levels following transient miRNA silencing in p53 WT and silenced (1.3 and 1.5-fold, respectively) HepG2 cells (**Figure S4A, B**). To assess if miR-30e-3p regulation of *MDM2* is long lasting, we evaluated its expression in miR-30e-3p stably silenced (MZIP-30e-3p) HepG2 cells and detected increased protein levels (**Figure S4C**), highlighting a prolonged post-transcriptional regulation. Finally, we verified miRNA/mRNA interaction by performing a reporter assay in HepG2 cells. MiR-30e-3p co-transfection decreased luciferase activity of WT MDM2-3'UTR vectors, but not that of mutant ones, proving miRNA direct interaction with its complementary sequence in *MDM2* mRNA (**Figure 3G)**. To verify the existence of a possible miR-30e/*MDM2*/*TP53* feedback loop, we measured p53 transcriptional activity and expression in WT and mutant *TP53*-bearing cells following miR-30e-3p overexpression. An increase of luciferase signal and p53 protein expression was registered in miR-30e-3p transfected HepG2 cells; whereas no change was observed in Huh-7 cells harboring an inactive p53 isoform (**Figure 3H, S4D**). These data demonstrated that, in p53 WT contexts, miR-30e-3p increases p53 expression and activity by targeting mdm2, leading to a feedforward loop sustained by p53-dependent transcription of miR-30e-3p itself. Conversely, in *TP53* mutated backgrounds this positive loop is hampered, suggesting that other targets might mediate miR-30e-3p functions in these contexts.

MiR-30e-3p influences cell proliferation and invasion of HCC cells by targeting *MDM2*, *PTEN* and *CDKN1B*/*p27*

The regulation of cell proliferation and invasion by miR-30 family members has been reported in tumors [40, 41]; nevertheless, miR-30e-3p, the most downregulated miR-30 member in our patient cohorts and preclinical model, was not previously studied. Besides *MDM2*, a

bioinformatics analysis highlighted *p27* and *PTEN* among miR-30e-3p hypothetic targets (**Figure S5A**). Due to their key role in hepatocarcinogenesis, it is conceivable that miR-30e-3p establishes multi-target networks driving HCC phenotype. QPCR and WB analyses in transfected HCC cells proved *p27* and *PTEN* inhibition by miR-30e-3p at mRNA and protein levels (**Figure S5B**). A reporter assay showed decreased luciferase activity of p27 and PTEN 3'UTR WT vectors upon miR-30e-3p overexpression, demonstrating that miR-30e-3p directly regulates these targets through mRNA degradation (**Figure S5C**).

We subsequently explored the effect of miR-30e-3p on HCC cell proliferation by dissecting the contribution of mdm2/p53 axis and PTEN/AKT pathway. In order to investigate the former, we performed the proliferation assay in *TP53* WT and p53-silenced HepG2 cells. Cell growth inhibition (1.2-fold) occurred upon miR-30e-3p enforced expression in *TP53* WT cells, whereas an increase of cell proliferation (1.4-fold) was detected in *TP53*-silenced HepG2 cells (**Figure 4A, B**), suggesting p53 as a pivotal factor modulating miR-30e-3p effect. The relevance of *PTEN* targeting on cell proliferation was next assessed in p53-silenced cells by evaluating *AKT* phosphorylation upon miR-30e-3p enforced expression. An increase of phospho-AKT occurred in both *TP53* WT and p53-silenced HepG2 cells highlighting AKT, beside p53, as pivotal factors mediating miR-30e-3p effects. We next assayed p53-mutated Huh-7 and p53-deleted Hep3B cells displaying high constitutive pten levels [20]. MiR-30e-3p overexpression increased proliferation of Huh-7 and Hep3B cells (1.9 and 2.1-fold, respectively). Enhanced AKT phosphorylation confirmed PTEN/AKT targeting as a trigger for proliferation in these non-functional p53 backgrounds (**Figure 4C, D**). To check whether p27 contributes to cell proliferation, we chose p53-mutated SNU475 cells displaying null pten levels [20]. MiR-30e-3p increased proliferation of SNU475 cells without changing phospho-AKT levels, but strongly decreasing p27 (**Figure 4E**). These findings support the crucial role of mdm2/p53, p27 and AKT in mediating miR-30e-3p regulation of cell proliferation. We hence analyzed cell cycle regulators p21 and p27 in miR-30e-3p overexpressing HCC cells. P21 modulation reflected p53

status, showing an increase in *TP53* WT HepG2 cells only, while it did not change in *TP53*-mutated cell lines (**Figure 4A-E**). Conversely, p27 downregulation was observed in all cell lines, confirming its targeting by miR-30e-3p (**Figure 4A-E**). Opposite proliferative changes induced by miR-30e-3p in HCC cell lines can be explained by its multi-target activity. Indeed, the inhibition of mdm2 prevents cell cycle acceleration through p53/p21 signaling in *TP53* WT contexts only. On the contrary, p27 and PTEN inhibition prevails in *TP53*-mutated/deleted backgrounds, leading to increased proliferation.

We next explored miR-30e-3p ability to modulate invasive properties of HepG2 and SNU449 cells. These cell lines were chosen due to high miR-30e-3p constitutive levels that allowed the investigation of miR-30e-3p stable silencing (**Figure S5D**) in a p53 WT (HepG2) and p53-mutated context (SNU449). No change was observed in miR-30e-3p silenced HepG2 cells, whereas decreased invasive and migratory potentials were detected in miRNA-silenced SNU449 cells (Student's t-test; $p<0.0001$) (**Figure 4F, S5E**). Despite decreased phospho-AKT levels in both cell lines, their different invasion capability highlights cell context as pivotal in driving miR-30e-3p influence on cell aggressiveness.

MiR-30e-3p influences stem cell properties of HCC cells through *EpCAM* targeting

We investigated miR-30e-3p driven changes on stemness in HCC and observed a negative correlation between miR-30e-3p and both AFP and EpCAM mRNAs in HCC patients (Pearson's correlation; R=-0.45 and -0.36, respectively) (**Figure 5A**) and cell lines (Pearson's correlation; R=-0.62) (**Figure S6A**). Analyzing HCCs according to *TP53* status, an even stronger correlation was observed in *TP53* mutated patients (Pearson's correlation; R=-0.78) (**Figure S6B)**, suggesting a stronger activity of miR-30e-3p in the absence of miR-30e-3p/mdm2/p53 regulatory loop. An opposite behavior was detected for pri-miR-30e that positively correlated with EpCAM mRNA (Pearson's correlation; R=0.39) (**Figure S6C**). Accordingly, a change of EpCAM mRNA

and immunophenotype was observed following miR-30e-3p modulation in HCC cells (**Figure 5B and S6D**). To investigate how miR-30e-3p influences stem cell properties, we interrogated bioinformatics algorithms and identified two hypothetical miRNA binding sites in EpCAM 3'UTR (**Figure S6E**). A decreased luciferase activity was observed for WT EpCAM-3'UTR vector in presence of miR-30e-3p overexpression (Student's t-test; p=0.00045), demonstrating a direct regulation of this target in HCC (**Figure 5C**). We next performed clonogenic and sphere formation assays in miR-30e-3p stably silenced (MZIP-30e-3p) p53 WT HepG2 and p53-mutated SNU449 cells (**Figure S5E, S6F**), chosen on the basis of their different stemness features (**Figure S6G**). The clonogenic assay displayed an increase of colony number (t-test; p=0.0005) and OD 595 (t-test; p=0.001) in MZIP-30e-3p HepG2 cells, whereas an opposite behavior was observed in SNU449 cells displaying a decreased colony number (t-test; p<0.0001) and OD 595 (t-test; p=0.025) in miR-30e-3p silenced cells (**Figure 5D, E**). Finally, we performed colony-forming unit and sphere formation assays in miR-30e-3p stably overexpressing Huh-7 cells exhibiting high stem cell characteristics and a mutated p53 isoform (**Figure S6F, G**). A decrease of colony and sphere number (t-test; p=0.0033 and p=0.010, respectively) was observed in miR-30e-3p-Huh-7 cells (**Figure 5F, G**). Similarly, miR-30e-3p silencing determined an increased sphere formation (Student's t-test; p<0.0001) in HepG2 cells (**Figure 5G, S6H**). Due to low expression of stem cell characteristics, SNU449 cells displayed no capability to sphere formation (**Figure S6I**). An increase of AFP and EpCAM levels was observed in MZIP-30e-3p HepG2-derived spheres, whereas their decrease was detected in pMXs-miR-30e-3p Huh-7-derived spheres (**Figure 5H**), confirming findings observed in HCC specimens and cell lines.

In primary HCCs, low miR-30e-3p expression associated with microvascular invasion (Student's t-test; p=0.012) and increased recurrence rate (log-rank test; p=0.027) (**Figure 5I, J**). These findings demonstrated that miR-30e-3p downregulation participates to boost stemness properties in HCC cells characterized by a stem-like phenotype.

MiR-30e-3p regulates treatment response in HCC preclinical models through *MDM2* and *PTEN* targeting

Due to the relevance of miR-30e-3p targets in stressful conditions and drug response, we evaluated apoptotic cell death in HepG2 and Huh-7 cells following starvation and doxorubicin or sorafenib treatment. Firstly, we considered *TP53* WT HepG2 cells and observed that miR-30e-3p overexpression had no effect in basal conditions (**Figure 6A**). On the contrary, it increased early apoptosis (2.3-fold) following serum deprivation and both early and late apoptosis (1.3 and 7.8-fold, respectively) in doxorubicin treated cells (**Figure 6B, C**), which is consistent with p53 activation in these conditions (**Figure S7A**). WB and caspase assay confirmed increased p53 expression, apoptotic markers and caspase-3/7 activity upon miR-30e-3p enforced expression in serum-deprived and doxorubicin treated HepG2 cells (**Figure 6C-E**).

Similarly, sorafenib increased early apoptosis (3.1-fold increase) in miR-30e-3p transfected HepG2 cells (**Figure 6F-H**). Since both sorafenib (**Figure S7A)** and miR-30e-3p induces p53 expression (**Figure 6G**), we wondered if p53 might account for increased apoptotic cell death in miR-30e-3p overexpressing cells. To prove a p53-dependent response, we performed the same assays in p53-silenced HepG2 cells. In this setting, miR-30e-3p overexpression decreased (4.2-fold) early apoptotic cells (**Figure 6I-K**), demonstrating the central role of p53 in triggering miR-30e-3p-mediated apoptosis. In agreement, miR-30e-3p overexpression in *TP53* deleted (CRISPR/Cas9 technology) HepG2 cells determined a resistance to both starvation and sorafenib (**Figure S7B-E**), confirming p53 as a determinant of miR-30e-3p duality in HCC. To demonstrate the relevance of *PTEN*/*AKT* axis in the absence of p53, we coupled miR-30e-3p inhibition with *PTEN* silencing in p53-deleted HepG2 cells. Annexin-V assay after sorafenib administration showed that *PTEN* inhibition decreases early apoptosis (1.5-fold) in miR-30e-3p

silenced/p53-knockout HepG2 cells confirming PTEN/AKT pathway as a driver of sorafenib-resistance in the absence of p53 (**Figure S7F, G**). Finally, since sorafenib triggers p27 in HepG2 cells (**Figure S7H**), we wondered whether p27 targeting by miR-30e-3p might influence sorafenib response. Strikingly, when both *TP53* and *PTEN* were inhibited, miR-30e-3p overexpression decreased early apoptotic cell population (1.4-fold) in sorafenib treated HepG2 cells, suggesting p27 participation to miR-30e-3p-mediated sorafenib resistance in p53-depleted cells (**Figure S7I)**. These findings confirm the importance of PTEN and p27 in driving miR-30e-3p-associated phenotype in *TP53* mutated backgrounds. In line, miR-30e-3p overexpression in *TP53* mutated Huh-7 cells determined a resistance to starvation, doxorubicin and sorafenib administration (**Figure S8A-H**) and high miR-30e-3p levels associated with increased tumor cell proliferation in sorafenib-treated Huh-7-dervived xenograft mice (**Figure S8I, J**), confirming its oncogenic role in p53-mutated cells.

In sorafenib-treated DEN-HCC rats, a downregulation of miR-30e-3p expression was found in 73% of nodules (Student's t-test; p=0.02) (**Figure 7A**). Sorafenib resistant tumors showed lower miR-30e-3p tissue levels (Student's t-test; p=0.004) (**Figure 7B**), suggesting miR-30e-3p downregulation as an adverse event with respect to sorafenib efficacy in this model. In agreement, an inverse correlation between miR-30e-3p and tumor size (Pearson's correlation; R=-0.69) (**Figure 7C**) and a positive correlation between miR-30e-3p and apoptotic markers (Pearson's correlation; R=0.70, 0.71 and 0.49) were identified in treated rat HCCs (**Figure S9A-C**). Finally, the positive correlation between miR-30e-3p and p21 levels in tumor tissues (Pearson's correlation; R=0.52) (**Figure S9D**) from *TP53* WT rat DEN-HCCs [42], led us to speculate that miR-30e-3p/mdm2/p53 axis might take part to sorafenib sensitization also in rat tumors.

Circulating miR-30e-3p levels predict treatment response in HCC

Circulating miRNAs were proposed as biomarkers of treatment response [43] and TKIs, such as gefitinib, promote exosomal secretion [44]. Thus, we assayed if sorafenib could modulate miR-30e-3p extracellular levels. An exosome-mediated miR-30e-3p extrusion was confirmed in all HCC cell lines treated by sorafenib, except for SNU449 cells. Sorafenib decreased intracellular miR-30e-3p levels in sensitive cell lines (HepG2, Hep3B and Huh-7), while it increased miRNA levels in the resistant (SNU475) one (**Figure 7D-F**). Aiming at identifying molecular mechanisms underneath miR-30e-3p extrusion triggered by sorafenib, we focused on p53, a known promoter of exosomal secretion [45]. We assayed p53 activity following sorafenib treatment in WT *TP53* HepG2 cells, in SNU475 cells that harbor a double *TP53* heterozygous mutation but maintain a residual *TP53* transcriptional activity and in SNU449 cells with a mutated and transcriptionally inactive *TP53* isoform (**Figure 3B**). Sorafenib increased *TP53* activity in both HepG2 and SNU475 cells, but not in SNU449 cells (**Figure 7G**). We next performed *TP53* silencing and deletion in HepG2 cells and observed that p53 absence prevented miR-30e-3p extracellular and exosomal rising (**Figure 7H and S9E**), confirming that p53 contributes to sorafenib-mediated miR-30e-3p exosomal secretion by HCC cells.

Remarkably, an inverse correlation between tissue and serum miR-30e-3p levels was detected in both DEN-HCC rats and xenograft mice subjected to sorafenib treatment (Pearson's correlation; R=-0.58 and R=-0.88, respectively) (**Figure S9F, G**). In addition, a negative correlation between miR-30e-3p circulating levels and apoptotic molecules was found in sorafenib-treated HCC rats (Pearson's correlation; R=-0.82, -0.65 and -0.51, respectively) (**Figure S9H-J**) and higher circulating miR-30e-3p levels were detected in sorafenib-resistant group (Student's t-test; p=0.05) (**Figure 7I**). Taken together, these correlative findings suggested miR-30e-3p as a potential biomarker of treatment response.

We thus tested circulating miR-30e-3p levels in patients with advanced HCC (**Table S2**), assaying sera samples collected before (46 patients, 25 responders and 21 non-responders at two months) and on sorafenib treatment (49 patients, 23 responders and 26 non-responders at the 4

468 months follow-up assessment). Circulating miR-30e-3p levels did not differ between responders
469 and non-responders (mean circulating miR-30e-3p: 2.24 in R vs 1.96 in NR; unpaired t-test,
470 p=0.3, **Figure 7J**) ruling out any predictor role of primary response. Conversely, higher
471 circulating miR-30e-3p was found at the two months follow-up in patients experiencing escape
472 to treatment at the four months TC (circulating miR-30e-3p at two months: 2.13 in responders vs
473 3.18 in non-responders, unpaired T-test, p<0.0001; **Figure 7K)**, suggesting its early elevation in
474 acquired drug resistance. In a subgroup of 28 patients (13 responders and 15 non-responders at
475 the four months follow-up), variations of circulating miR-30e-3p were tested over time (basal
476 versus two months follow-up). Even though the cohort is small, preventing any conclusion, an
477 increase in circulating miR-30e-3p levels at the two months assessment was observed in patients
478 developing escape at the subsequent CT-scan (**Figure S9K, L***)*. Notably, circulating miR-30e-5p
479 levels did not predict sorafenib response neither before nor on treatment (**Figure S9M, N**)
480 further highlighting the specificity of miR-30e-3p variations in acquired resistance to sorafenib.
481 In conclusion, even though these data are very preliminary and circumstantial, the early rising of
482 circulating miR-30e-3p in patients developing sorafenib resistance makes this miRNA appealing
483 for further exploitation, in a field where non-invasive biomarkers are needed.

Discussion

MiRNAs act as tumor suppressors (TS) or oncogenes depending on targets' core, driver gene mutations and tumor microenvironment. Here we report the downregulation of miR-30e-3p in human and rat HCCs and its association with poor prognosis, proliferation, stemness phenotype and drug resistance. The modulation of different biological functions has to be ascribed to the simultaneous targeting of both oncogenes and tumor suppressor genes.

Previous studies reported miR-30 as a 'dual' miRNA, with opposite functions in NSCLC and pancreatic cancer [15, 18]. Here, we describe the 'dual' role of miR-30e-3p within the same tumor type, highlighting opposite effects based on different molecular backgrounds and in particular to *TP53* status. On one hand, miR-30e-3p decreased cell proliferation and induced sorafenib sensitization in *TP53* WT HepG2 cells, behaving as a TS miRNA. On the other hand, it induced proliferation, and drug resistance in *TP53*-mutated/deleted HCC cells, behaving as an oncomiR. Indeed, both tumor suppressors (*CDKN1B*/*p27* and *PTEN*) and oncogenes (*MDM2, EpCAM*) were demonstrated to be miR-30e-3p targets. Specifically, miR-30e-3p exerts TS functions in *TP53* WT contexts where mdm2 targeting is prevalent, leading to p53 pathway activation. On the contrary, tumor-promoting effects take place in non-functional p53 contexts, where p27 and PTEN targeting becomes prevalent. In particular, p27 drives the proliferating phenotype; EpCAM modulates staminal properties, whereas PTEN contributes to drug resistance by triggering AKT activation [46]. Similarly, we previously reported a dual behavior for miR-221 with respect to p53 status, highlighting the importance of molecular characterization when antagomiR strategies are considered [21]. Indeed, both miR-221 and miR-30e-3p modulate the *TP53* axis through mdm2 direct regulation explaining, at least in part, their opposite activity in different *TP53* contexts.

As established for miR-30a and miR-30e-5p [24, 25] here we proved that p53 activates miR-30e transcription. Nevertheless, we observed a negative correlation between primary and mature

miR-30e-3p levels, envisaging regulatory events on miRNA biogenesis. Strikingly, mature but not primary miRNA profiles clustered normal and tumor samples into separate nodes, suggesting maturation processes as more relevant than altered transcription for aberrant miRNA expression [47]. Gain-of-function of mutated p53 isoforms hampers miRNA processing machinery leading to miRNA downregulation due to interference with both p68 and p72/82 RNA helicases, impairing Drosha microprocessor activity [23, 48]. Moreover, R273H mutated p53 inhibits miR-30a transcription contributing to its aberrant expression in breast cancer [49]. We observed an association between p53 mutations and miR-30e-3p downregulation, as well as the inhibition of miRNA maturation following Nutlin-3 treatment, suggesting the enrollment of other mdm2 targets, such as p53 family members (p63 and p73), as possible regulators of miRNA biogenesis. In this regard, an elegant study by Su and coworkers demonstrated that Dicer1 is a transcriptional target of TAp63 but not of p53 [50]. Our descriptive findings on p53 involvement in miRNA biogenesis led us to speculate that p53 accumulation, as in the case of *MDM2* permanent inhibition by Nutlin-3, might be responsible for the transcriptional inhibition of Dicer1 through saturation of p63/p53-REs, preventing p63-mediated transcription. Dicer1 disruption in knockout (KO) mice promoted hepatocarcinogenesis and led to the deregulation of several miRNAs, including all miR-30 family members, suggesting a strict regulation of miR-30 maturation by Dicer1 in HCC [51].

Rat HCCs, characterized by a *TP53* WT background [42], showed an inverse correlation between miR-30e-3p and tumor size, as well as reduced miR-30e-3p tissue levels in sorafenib resistant tumors, suggesting miR-30e-3p downregulation as a contributor to sorafenib resistance. New molecules, beside sorafenib, were recently registered for advanced HCC [52], however biomarkers predicting treatment outcome are lacking. In the last two decades, miRNAs have emerged as attractive diagnostic, prognostic and therapeutic tools [53, 54] and reliable markers [43]. Decreased miR-30e and miR-223 serum levels were reported in HCC patients irrespective

of tumor etiology [55], whereas miR-30e-enriched vesicles decreased mesenchymal properties in cholangiocarcinoma cells [56].

Our and other groups reported sorafenib as a trigger for *TP53* activation and demonstrated *TP53* as a key player for exosomal secretion in stressful conditions [45] even though mechanisms governing exosomal secretion remain poorly understood. Here we confirmed the contribution of the p53 pathway to miR-30e-3p exosomal secretion in sorafenib-treated HCC cell lines. In addition, as reported for the TKI gefitinib, sorafenib triggers exosome secretion in HCC cells [44]. Increased miR-30e-3p circulating levels were found in sorafenib resistant rat and human HCCs. In particular, higher miR-30e-3p circulating levels, deriving from exosomal secretion, were associated with subsequent escape to sorafenib. This does not prove a causative effect and may simple represent a bystander event; however, miR-30e-3p role as a non-invasive predictor of treatment escape can be envisaged and should be further investigated in larger patient cohorts.

Acknowledgements and Financial Support Statement

We thank Dr. Vilma Mantovani and Dr. Marinella Cenci of Genitics Unit at S.Orsola-Malpighi University Hospital for cell line authentication. We thank Dr. Clarissa Patrizi of Modena and Reggio Emilia University for her precious help with CRISPR technology.

Financial support: (1) Programma di Ricerca Regione-Università, Regione Emilia-Romagna, Bando "Alessandro Liberati", to F.F. "Identification of innovative microRNAs-based biomarkers and anti-cancer strategies for the treatment of Hepatocellular carcinoma". (2) Programma di Ricerca Regione-Università, Regione Emilia-Romagna, Bando "Ricerca Innovativa", to L.B. and L.G. "Innovative approaches to the diagnosis and pharmacogenetic-based therapies of primary hepatic tumors, peripheral B and T-cell lymphomas and lymphoblastic leukaemias".

References

1. Llovet JM, Zucman-Rossi J, Pikarsky E, Sangro B, Schwartz M, Sherman M, et al. Hepatocellular carcinoma. Nat Rev Dis Primers 2016;**2**:16018.

2. Llovet JM, Villanueva A, Lachenmayer A, Finn RS. Advances in targeted therapies for hepatocellular carcinoma in the genomic era. Nat Rev Clin Oncol 2015;**12**:408-24.

3. Colombo F, Baldan F, Mazzucchelli S, Martin-Padura I, Marighetti P, Cattaneo A, et al. Evidence of distinct tumour-propagating cell populations with different properties in primary human hepatocellular carcinoma. Plos One 2011;**6**:e21369.

4. Volinia S, Calin GA, Liu CG, Ambs S, Cimmino A, Petrocca F, et al. A microRNA expression signature of human solid tumors defines cancer gene targets. PNAS 2006;**103**:2257-61.

5. Zhang B, Pan X, Cobb GP, Anderson TA. microRNAs as oncogenes and tumor suppressors. Dev Biol 2007;**302**:1-12.

6. Budhu A, Jia HL, Forgues M, Liu CG, Goldstein D, Lam A, et al. Identification of metastasis-related microRNAs in hepatocellular carcinoma. Hepatology 2008;**47**:897-907.

7. Gramantieri L, Fornari F, Ferracin M, Veronese A, Sabbioni S, Calin GA, et al. MicroRNA-221 targets Bmf in hepatocellular carcinoma and correlates with tumor multifocality. Clin Cancer Res 2009;**15**:5073-81.

8. Bai S, Nasser MW, Wang B, Hsu SH, Datta J, Kutay H, et al. MicroRNA-122 inhibits tumorigenic properties of hepatocellular carcinoma cells and sensitizes these cells to sorafenib. J Biol Chem 2009;**284**:32015-27.

9. Fornari F, Pollutri D, Patrizi C, La Bella T, Marinelli S, Casadei Gardini A, et al. In Hepatocellular Carcinoma miR-221 Modulates Sorafenib Resistance through Inhibition of Caspase-3-Mediated Apoptosis. Clin Cancer Res 2017;**23**:3953-65.

582 10. Garofalo M, Di Leva G, Romano G, Nuovo G, Suh SS, Ngankeu A, et al. miR-221&222
583 regulate TRAIL resistance and enhance tumorigenicity through PTEN and TIMP3
584 downregulation. Cancer Cell 2009;**16**:498-509.
585 11. Ichimi T, Enokida H, Okuno Y, Kunimoto R, Chiyomaru T, Kawamoto K, et al.
586 Identification of novel microRNA targets based on microRNA signatures in bladder cancer. Int J
587 Cancer 2009;**125**:345-52.
588 12. Zhao JJ, Lin J, Zhu D, Wang X, Brooks D, Chen M, et al. miR-30-5p functions as a
589 tumor suppressor and novel therapeutic tool by targeting the oncogenic Wnt/beta-catenin/BCL9
590 pathway. Cancer Res 2014;**74**:1801-13.
591 13. Volinia S, Galasso M, Costinean S, Tagliavini L, Gamberoni G, Drusco A, et al.
592 Reprogramming of miRNA networks in cancer and leukemia. Genome Res 2010;**20**:589-99.
593 14. Chen Z, Zhang J, Zhang Z, Feng Z, Wei J, Lu J, et al. The putative tumor suppressor
594 microRNA-30a-5p modulates clear cell renal cell carcinoma aggressiveness through repression
595 of ZEB2. Cell Death Dis 2017;**8**:e2859.
596 15. Kumarswamy R, Mudduluru G, Ceppi P, Muppala S, Kozlowski M, Niklinski J, et al.
597 MicroRNA-30a inhibits epithelial-to-mesenchymal transition by targeting Snai1 and is
598 downregulated in non-small cell lung cancer. Int J Cancer 2012;**130**:2044-53.
599 16. Zhang Q, Yu L, Qin D, Huang R, Jiang X, Zou C, et al. Role of microRNA-30c targeting
600 ADAM19 in colorectal cancer. PloS One 2015;**10**:e0120698.
601 17. Su W, Hong L, Xu X, Huang S, Herpai D, Li L, et al. miR-30 disrupts senescence and
602 promotes cancer by targeting both p16(INK4A) and DNA damage pathways. Oncogene
603 2018;**37**:5618-32.
604 18. Tsukasa K, Ding Q, Miyazaki Y, Matsubara S, Natsugoe S, Takao S. miR-30 family
605 promotes migratory and invasive abilities in CD133(+) pancreatic cancer stem-like cells. Hum
606 cell 2016;29:130-7.

19. Shimada S, Mogushi K, Akiyama Y, Furuyama T, Watanabe S, Ogura T, et al. Comprehensive and integrative genomic characterization of HCC. EBiomedicine 2019;**40**:457-70.

20. Fornari F, Milazzo M, Chieco P, Negrini M, Marasco E, Capranico G, et al. In hepatocellular carcinoma miR-519d is up-regulated by p53 and DNA hypomethylation and targets CDKN1A/p21, PTEN, AKT3 and TIMP2. J Pathol 2012;**227**:275-85.

21. Fornari F, Milazzo M, Galassi M, Callegari E, Veronese A, Miyaaki H, et al. p53/mdm2 feedback loop sustains miR-221 expression and dictates the response to anticancer treatments in hepatocellular carcinoma. Mol Cancer Res 2014;**12**:203-16.

22. Raver-Shapira N, Marciano E, Meiri E, Spector Y, Rosenfeld N, Moskovits N, et al. Transcriptional activation of miR-34a contributes to p53-mediated apoptosis. Mol Cell 2007;**26**:731-43.

23. Suzuki HI, Yamagata K, Sugimoto K, Iwamoto T, Kato S, Miyazono K. Modulation of microRNA processing by p53. Nature 2009;**460**:529-33.

24. di Gennaro A, Damiano V, Brisotto G, Armellin M, Perin T, Zucchetto A, et al. A p53/miR-30a/ZEB2 axis controls triple negative breast cancer aggressiveness. Cell Death Differ 2018;**25**:2165-80.

25. Laudato S, Patil N, Abba ML, Leupold JH, Benner A, Gaiser T, et al. P53-induced miR-30e-5p inhibits colorectal cancer invasion and metastasis by targeting ITGA6 and ITGB1. Int J Cancer 2017;**141**:1879-90.

26. Deng L, Tang J, Yang H, Cheng C, Lu S, Jiang R, et al. MTA1 modulated by miR-30e contributes to epithelial-to-mesenchymal transition in hepatocellular carcinoma through an ErbB2-dependent pathway. Oncogene 2017;**36**:3976-85.

27. Liu Z, Tu K, Liu Q. Effects of microRNA-30a on migration, invasion and prognosis of hepatocellular carcinoma. FEBS Lett 2014;**588**:3089-97.

632 28. Yao J, Liang L, Huang S, Ding J, Tan N, Zhao Y, et al. MicroRNA-30d promotes tumor
633 invasion and metastasis by targeting Galphai2 in hepatocellular carcinoma. Hepatology
634 2010;**51**:846-56.
635 29. Hand NJ, Master ZR, Eauclaire SF, Weinblatt DE, Matthews RP, Friedman JR. The
636 microRNA-30 family is required for vertebrate hepatobiliary development. Gastroenterology
637 2009;**136**:1081-90.
638 30. Gramantieri L, Ferracin M, Fornari F, Veronese A, Sabbioni S, Liu CG, et al. Cyclin G1
639 is a target of miR-122a, a microRNA frequently down-regulated in human hepatocellular
640 carcinoma. Cancer Res 2007;**67**:6092-9.
641 31. Fornari F, Ferracin M, Trere D, Milazzo M, Marinelli S, Galassi M, et al. Circulating
642 microRNAs, miR-939, miR-595, miR-519d and miR-494, Identify Cirrhotic Patients with HCC.
643 PloS One. 2015;**10**:e0141448.
644 32. Fornari F, Gramantieri L, Giovannini C, Veronese A, Ferracin M, Sabbioni S, et al. MiR-
645 122/cyclin G1 interaction modulates p53 activity and affects doxorubicin sensitivity of human
646 hepatocarcinoma cells. Cancer Res 2009;**69**:5761-7.
647 33. Fornari F, Milazzo M, Chieco P, Negrini M, Calin GA, Grazi GL, et al. MiR-199a-3p
648 regulates mTOR and c-Met to influence the doxorubicin sensitivity of human hepatocarcinoma
649 cells. Cancer Res 2010;**70**:5184-93.
650 34. Pollutri D, Patrizi C, Marinelli S, Giovannini C, Trombetta E, Giannone FA, et al. The
651 epigenetically regulated miR-494 associates with stem-cell phenotype and induces sorafenib
652 resistance in hepatocellular carcinoma. Cell Death Dis 2018;**9**:4.
653 35. Fittipaldi S, Vasuri F, Bonora S, Degiovanni A, Santandrea G, Cucchetti A, et al. miRNA
654 Signature of Hepatocellular Carcinoma Vascularization: How the Controls Can Influence the
655 Signature. Dig Dis Sci 2017;**62**:2397-407.
656 36. Pollutri D, Gramantieri L, Bolondi L, Fornari F. TP53/MicroRNA Interplay in
657 Hepatocellular Carcinoma. Int J Mol Sci 2016;**17**(12).

658 37. He L, He X, Lim LP, de Stanchina E, Xuan Z, Liang Y, et al. A microRNA component of
659 the p53 tumour suppressor network. Nature 2007;**447**:1130-4.
660 38. Boominathan L. The tumor suppressors p53, p63, and p73 are regulators of microRNA
661 processing complex. PloS One 2010;**5(**5):e10615.
662 39. Ozsolak F, Poling LL, Wang Z, Liu H, Liu XS, Roeder RG, et al. Chromatin structure
663 analyses identify miRNA promoters. Genes Dev 2008;**22**:3172-83.
664 40. Ning ZQ, Lu HL, Chen C, Wang L, Cai W, Li Y, et al. MicroRNA-30e reduces cell
665 growth and enhances drug sensitivity to gefitinib in lung carcinoma. Oncotarget 2017;**8**:4572-81.
666 41. Schepeler T, Holm A, Halvey P, Nordentoft I, Lamy P, Riising EM, et al. Attenuation of
667 the beta-catenin/TCF4 complex in colorectal cancer cells induces several growth-suppressive
668 microRNAs that target cancer promoting genes. Oncogene 2012;**31**:2750-60.
669 42. Sasaki Y, Tsujiuchi T, Murata N, Kubozoe T, Tsutsumi M, Konishi Y. Absence of p16,
670 p21 and p53 gene alterations in hepatocellular carcinomas induced by N-nitrosodiethylamine or
671 a choline-deficient L-amino acid-defined diet in rats. Cancer Lett 2000;**152**:71-7.
672 43. Mitchell PS, Parkin RK, Kroh EM, Fritz BR, Wyman SK, Pogosova-Agadjanyan EL, et
673 al. Circulating microRNAs as stable blood-based markers for cancer detection. PNAS
674 2008;**105**:10513-8.
675 44. Li XQ, Liu JT, Fan LL, Liu Y, Cheng L, Wang F, et al. Exosomes derived from gefitinib-
676 treated EGFR-mutant lung cancer cells alter cisplatin sensitivity via up-regulating autophagy.
677 Oncotarget 2016;**7**:24585-95.
678 45. Yu X, Harris SL, Levine AJ. The regulation of exosome secretion: a novel function of the
679 p53 protein. Cancer Res 2006;**66**:4795-801.
680 46. Chen KF, Chen HL, Tai WT, Feng WC, Hsu CH, Chen PJ, et al. Activation of
681 phosphatidylinositol 3-kinase/Akt signaling pathway mediates acquired resistance to sorafenib in
682 hepatocellular carcinoma cells. J Pharmacol Exp Ther 2011;**337**:155-61.

683 47. Thomson JM, Newman M, Parker JS, Morin-Kensicki EM, Wright T, Hammond SM.
684 Extensive post-transcriptional regulation of microRNAs and its implications for cancer. Genes
685 Dev 2006;**20**:2202-7.
686 48. Garibaldi F, Falcone E, Trisciuoglio D, Colombo T, Lisek K, Walerych D, et al. Mutant
687 p53 inhibits miRNA biogenesis by interfering with the microprocessor complex. Oncogene
688 2016;**35**:3760-70.
689 49. Guo F, Chen H, Chang J, Zhang L. Mutation R273H confers p53 a stimulating effect on
690 the IGF-1R-AKT pathway via miR-30a suppression in breast cancer. Biomed Pharmacother
691 2016;**78**:335-41.
692 50. Su X, Chakravarti D, Cho MS, Liu L, Gi YJ, Lin YL, et al. TAp63 suppresses metastasis
693 through coordinate regulation of Dicer and miRNAs. Nature 2010;**467**:986-90.
694 51. Sekine S, Ogawa R, Ito R, Hiraoka N, McManus MT, Kanai Y, et al. Disruption of
695 Dicer1 induces dysregulated fetal gene expression and promotes hepatocarcinogenesis.
696 Gastroenterology 2009;**136**:2304-15 e1-4.
697 52. Kudo M. A New Era of Systemic Therapy for Hepatocellular Carcinoma with
698 Regorafenib and Lenvatinib. Liver Cancer 2017;**6**:177-84.
699 53. Janssen HL, Reesink HW, Lawitz EJ, Zeuzem S, Rodriguez-Torres M, Patel K, et al.
700 Treatment of HCV infection by targeting microRNA. New Engl J Med 2013;**368**:1685-94.
701 54. Rupaimoole R, Slack FJ. MicroRNA therapeutics: towards a new era for the management
702 of cancer and other diseases. Nat Rev Drug Dis 2017;**16**:203-22.
703 55. Bhattacharya S, Steele R, Shrivastava S, Chakraborty S, Di Bisceglie AM, Ray RB.
704 Serum miR-30e and miR-223 as Novel Noninvasive Biomarkers for Hepatocellular Carcinoma.
705 Am J Pathol 2016;**186**:242-7.
706 56. Ota Y, Takahashi K, Otake S, Tamaki Y, Okada M, Aso K, et al. Extracellular vesicle-
707 encapsulated miR-30e suppresses cholangiocarcinoma cell invasion and migration via inhibiting
708 epithelial-mesenchymal transition. Oncotarget 2018;**9**:16400-17.

Figure Legends

Figure 1. Deregulated expression of miR-30 family in human and rat HCCs. (**A-C**) Box plot graphs of miR-30e-3p, miR-30e-5p and miR-30a-3p in human and (**D-F**) rat tumor and non-tumor (NT) samples or liver cirrhosis (LC). (**G-I**) Box plot graph of miR-30e-3p, miR-30e-5p and miR-30a-3p in the validation cohort and in normal livers (NL). On the top of each graph is reported the p-value relative to ANOVA, whereas stars represent comparison between groups (Tukey's post hoc test). (**J, K**) Box plot graphs of mature and primary (pri-miR) miR-30e-3p in wild type (WT) and mutated (MUT) *TP53* HCC specimens. Y-axes report $2^{-\Delta\Delta Ct}$ values corresponding to miRNA levels.

Figure 2. *TP53* regulates miR-30e expression in HCC cells. (**A**) QPCR analysis of primary miR-30e (pri-miR-30e) and mature isoforms (miR-30e-3p, miR-30e-5p, miR-34a) in *TP53* silenced, (**B**) *TP53* overexpressing (pCMV-p53) and (**C**) Nutlin-3 treated HepG2 cells or (**D-E**) Nutlin-3 treated p53-deleted HepG2 (CRISPR) and p53-null Hep3B cells. (**F**) QPCR analysis of primary miR-30e and mature isoforms in *TP53* overexpressing Hep3B cells and (**G**) mutated *TP53* (pBabe-p53-mut) overexpressing HepG2 cells. (**A-G**) WB and qPCR analyses of *TP53*, *MDM2*, *CDKN1A/p21* in the same settings. U6RNA and β-actin were used as housekeeping genes. QPCR experiments were performed twice in triplicate; p-values from unpaired t-test are shown in each graph. Scr: scramble oligonucleotide; pCMV and pBabe: control vectors; DMSO: vehicle.

Figure 3. MiR-30e-3p targets *MDM2* in HCC cells. (**A**) MiR-30e-3p hypothetical binding sites in *MDM2* 3'UTR, as identified by Targetscan. Stars represent mutated bases. (**B**) QPCR analysis of miR-30e-3p in HCC, liver cirrhosis (LC) and normal liver (NL) as well as in HCC cell lines.

TP53 status and relative transcriptional activity are reported in the table below the graph, *TP53* activity has been normalized on that detected in HepG2 cells. (**C-E**) QPCR and WB analyses of miRNA and *MDM2* expression in miR-30e-3p overexpressing Huh-7, Hep3B and SNU475 cells and (**F**) miR-30e-3p silenced SNU449 cells. Time after transfection: 24 h. Y-axes represent relative expression levels. U6RNA and β-actin were used as housekeeping genes. (**G**) Luciferase reporter assay in HepG2 cells co-transfected with wild type (WT) or mutated (MUT) pGL3-MDM2-3UTR vectors and miR-30e-3p or negative control (NC). This experiment was repeated three times in triplicate. (**H**) P53 reporter assay and WB analysis in miR-30e-3p overexpressing HepG2 and Huh-7 cells. (**G, H**) Y-axes report relative values with respect to negative controls. NC: pre-miR negative control; NCi: anti-miR negative control; AM-30e-3p: anti-miR-30e-3p.

Figure 4. MiR-30e-3p influences cell growth and invasion of HCC cells. (**A, B**) Growth curves of miR-30e-3p and negative control (NC) transfected HepG2 cells in basal conditions and following p53 silencing. (**C-E**) Growth curves of miR-30e-3p transfected Huh-7, Hep3B and SNU475 cells with respect to negative control (NC) cells. (**A-E**) WB analysis of p53, PTEN, pAKT, p27 and p21 levels normalized on β-actin housekeeping gene. (**F**) Real time invasion assay of miR-30e-3p stably silenced (MZIP-30e-3p) HepG2 and SNU449 cells with respect to controls (MZIP-shRNA).

Figure 5. MiR-30e-3p influences stem cell properties of HCC cells. (**A**) Correlation graphs between miR-30e-3p and AFP or EpCAM mRNAs in HCC patients (N=30). Axes report $2^{-\Delta\Delta Ct}$ values transformed in a log2 form. (**B**) QPCR analysis of EpCAM expression in miR-30e-3p overexpressing Huh-7 cells (transient transfection) and miR-30e-3p silenced HepG2 cells (stable infection). Y-axis reports relative gene expression. (**C**) Luciferase reporter assay in HepG2 cells

co-transfected with WT or mutated (MUT) pGL3-EpCAM-3UTR vectors and miR-30e-3p or negative control (NC). (**D-F**) Six-well plate images of clonogenic assay in MIZ-30e-3p and control (MZIP-shRNA) HepG2 and SNU449 cells, as well as in miR-30e-3p overexpressing (pMXs-miR-30e-3p) and control (pMXs-shRNA) Huh-7 cells. Column graphs represent colony count and OD 595. Columns and bars represent average ± SD values. (**G**) Sphere formation assay in MZIP-30e-3p and control HepG2 cells as well as in pMXs-miR-30e-3p and control (pMXs-shRNA) Huh-7 cells. Average ± SD values from two independent experiments are shown. (**H**) WB analysis of stemness markers in MZIP-30e-3p HepG2 and pMXs-miR-30e-3p Huh-7 spheres. (**I**) Box plot graph displaying miR-30e-3p expression in patients with or without microvascular invasion (MVI). (**J**) Kaplan-Meier survival curve in HCC patients with high or low miR-30e-3p expression. High or low miRNA values were considered with respect to median value.

Figures 6. MiR-30e-3p induces drug sensitization in HepG2 cells. (**A**) Annexin-V assay in untreated or (**B**) serum deprived (60h) miR-30e-3p overexpressing and control cells. (**C-E**) Annexin-V images, WB analysis and caspase activity assay in miR-30e-3p overexpressing cells following doxorubicin (2.0 µg/ml, 48h) or (**F-H**) sorafenib treatment (7.5 µM, 48h). (**I-K**) Annexin-V images, WB analysis and caspase activity assay in p53-silenced miR-30e-3p overexpressing HepG2 cells following sorafenib treatment.

Figure 7. Increased miR-30e-3p serum levels associate with sorafenib escape in HCC. (**A**) Box plot graph displaying miR-30e-3p levels in sorafenib-treated rat HCCs with respect to surrounding livers or (**B**) in responder (R) and non-responder (NR) groups. (**C**) Correlation graph between tissue miR-30e-3p levels and tumor size in sorafenib-treated rat HCCs. (**D**)

QPCR analysis of intracellular, (**E**) extracellular and (**F**) exosomal miR-30e-3p levels in untreated and sorafenib treated HCC cells. Y-axes report relative values with respect to not-treated cells. DMSO was used as vehicle in untreated cells. Numbers below histograms represent relative cell viability values (%) of sorafenib treated versus untreated cells (48 h) identifying sensitive and resistant cell lines. (**G**) *TP53* activity assay in sorafenib treated HepG2, SNU449 and SNU475 cell lines (5 µM for 48 h). Y-axis reports relative p53 activity with respect to untreated cells (vehicle: DMSO). (**H**) QPCR analysis of intracellular, extracellular and exosomal miR-30e-3p levels in scramble and p53-silenced HepG2 cells after sorafenib treatment (5 µM for 48 h). U6RNA and cel-miR-39 were used as housekeeping genes for intracellular and extracellular/exosomal miRNA levels, respectively. Y-axis reports relative values with respect to not-treated cells. (**I**) Box plot graph displaying circulating miR-30e-3p levels in responder (R) and non-responder (NR) animals. (**J**) Box plot graph displaying circulating miR-30e-3p levels in serum samples from responder and non-responder HCC patients collected before treatment start and (**K**) at two-month follow-up. Response/escape to sorafenib was assessed at the subsequent (2-months or 4 months respectively) TC scan. Axes report $2^{-\Delta\Delta Ct}$ values transformed in a log2 form.

Figure 1

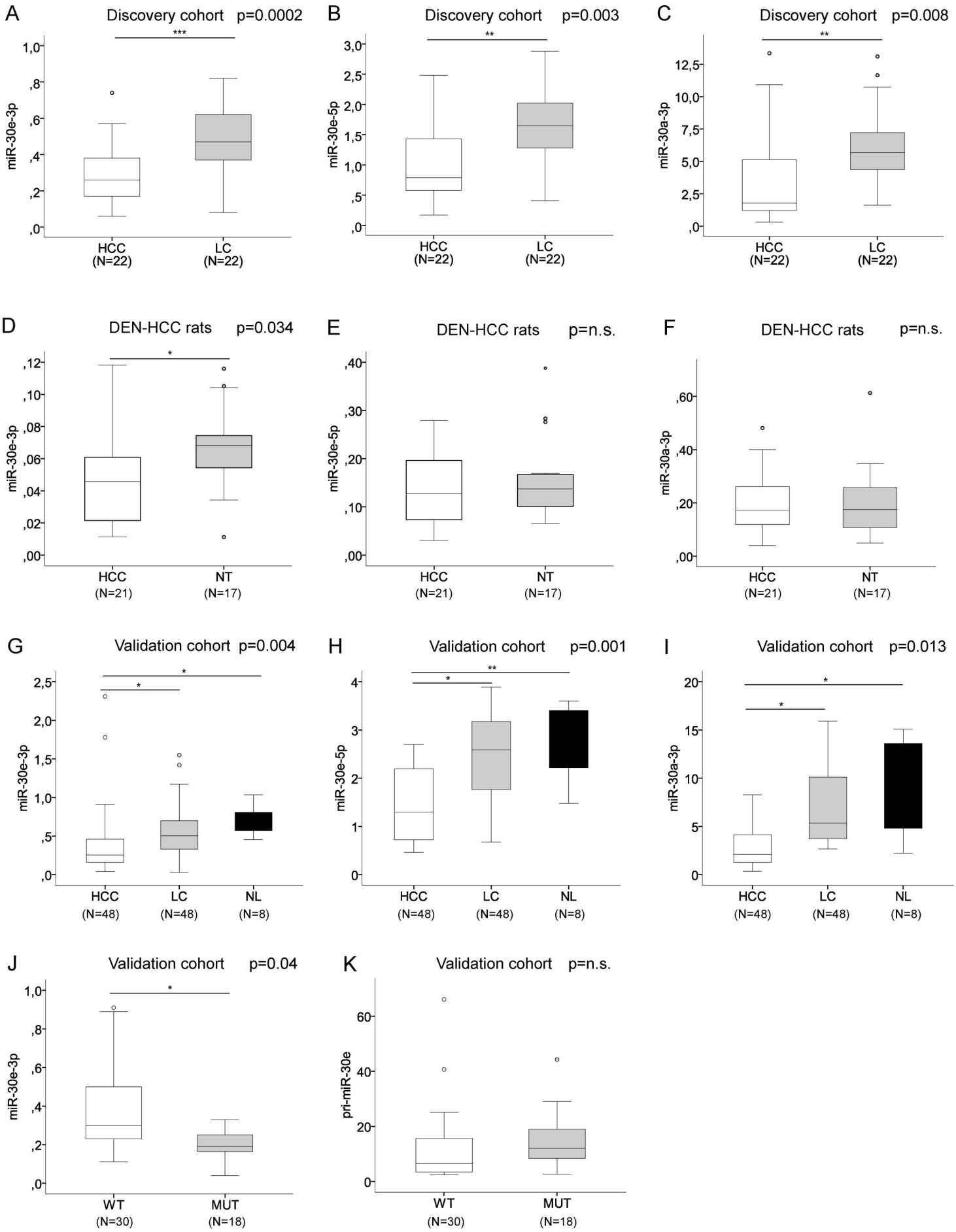
A
Discovery cohort p=0.0002
***
miR-30e-3p
1,0
,8
,6
,4
,2
,0
HCC (N=22)
LC (N=22)
B
Discovery cohort p=0.003
**
miR-30e-5p
3,0
2,5
2,0
1,5
1,0
,5
,0
HCC (N=22)
LC (N=22)
C
Discovery cohort p=0.008
**
miR-30a-3p
12,5
10,0
7,5
5,0
2,5
,0
HCC (N=22)
LC (N=22)
D
DEN-HCC rats p=0.034
*
miR-30e-3p
,12
,10
,08
,06
,04
,02
,00
HCC (N=21)
NT (N=17)
E
DEN-HCC rats p=n.s.
miR-30e-5p
,40
,30
,20
,10
,00
HCC (N=21)
NT (N=17)
F
DEN-HCC rats p=n.s.
miR-30a-3p
,60
,40
,20
,00
HCC (N=21)
NT (N=17)
G
Validation cohort p=0.004
*
*
miR-30e-3p
2,5
2,0
1,5
1,0
,5
,0
HCC (N=48)
LC (N=48)
NL (N=8)
H
Validation cohort p=0.001
**
*
miR-30e-5p
4
3
2
1
0
HCC (N=48)
LC (N=48)
NL (N=8)
I
Validation cohort p=0.013
*
*
miR-30a-3p
20
15
10
5
0
HCC (N=48)
LC (N=48)
NL (N=8)
J
Validation cohort p=0.04
*
miR-30e-3p
1,0
,8
,6
,4
,2
,0
WT (N=30)
MUT (N=18)
K
Validation cohort p=n.s.
pri-miR-30e
60
40
20
0
WT (N=30)
MUT (N=18)

Figure 2

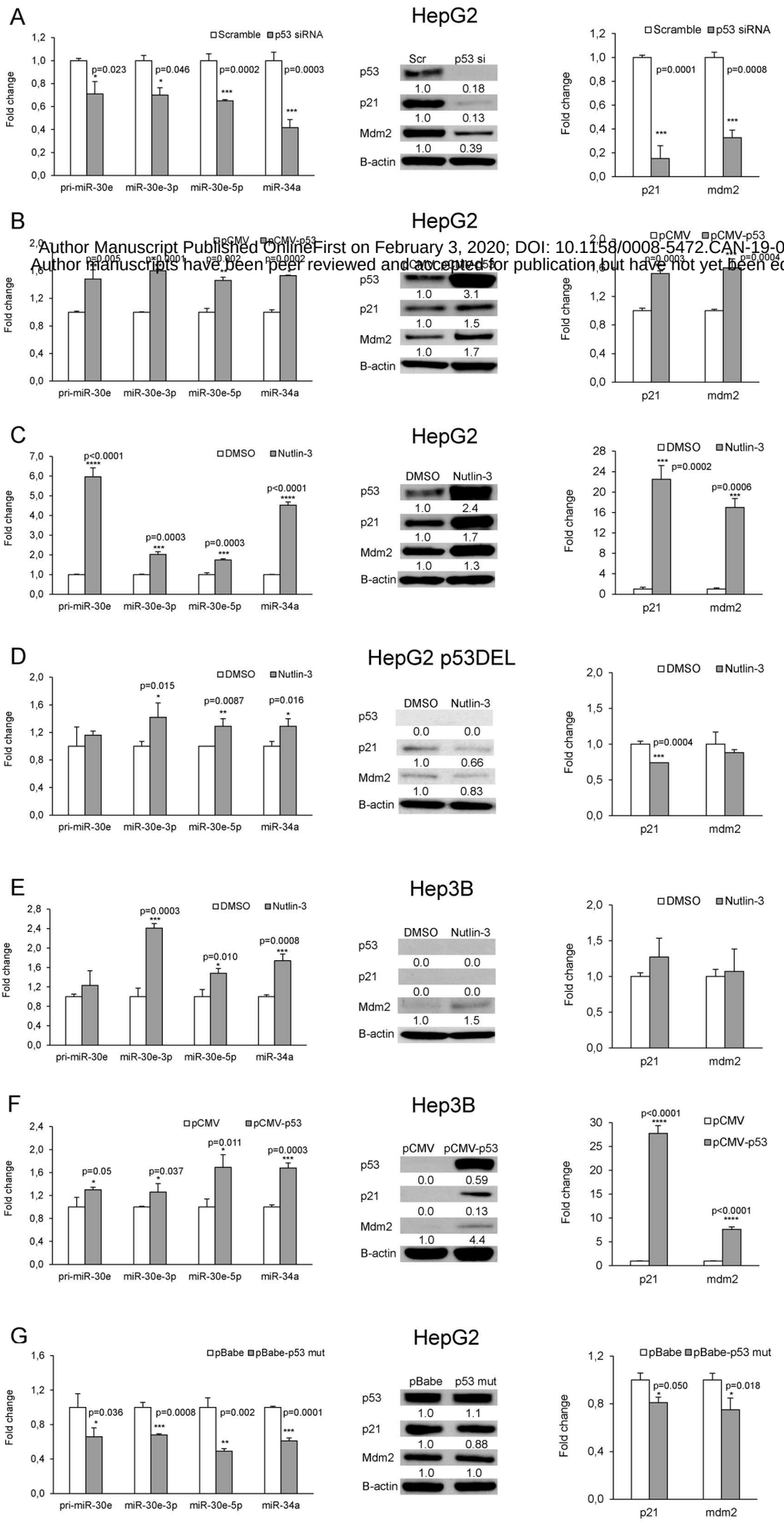

Figure 3

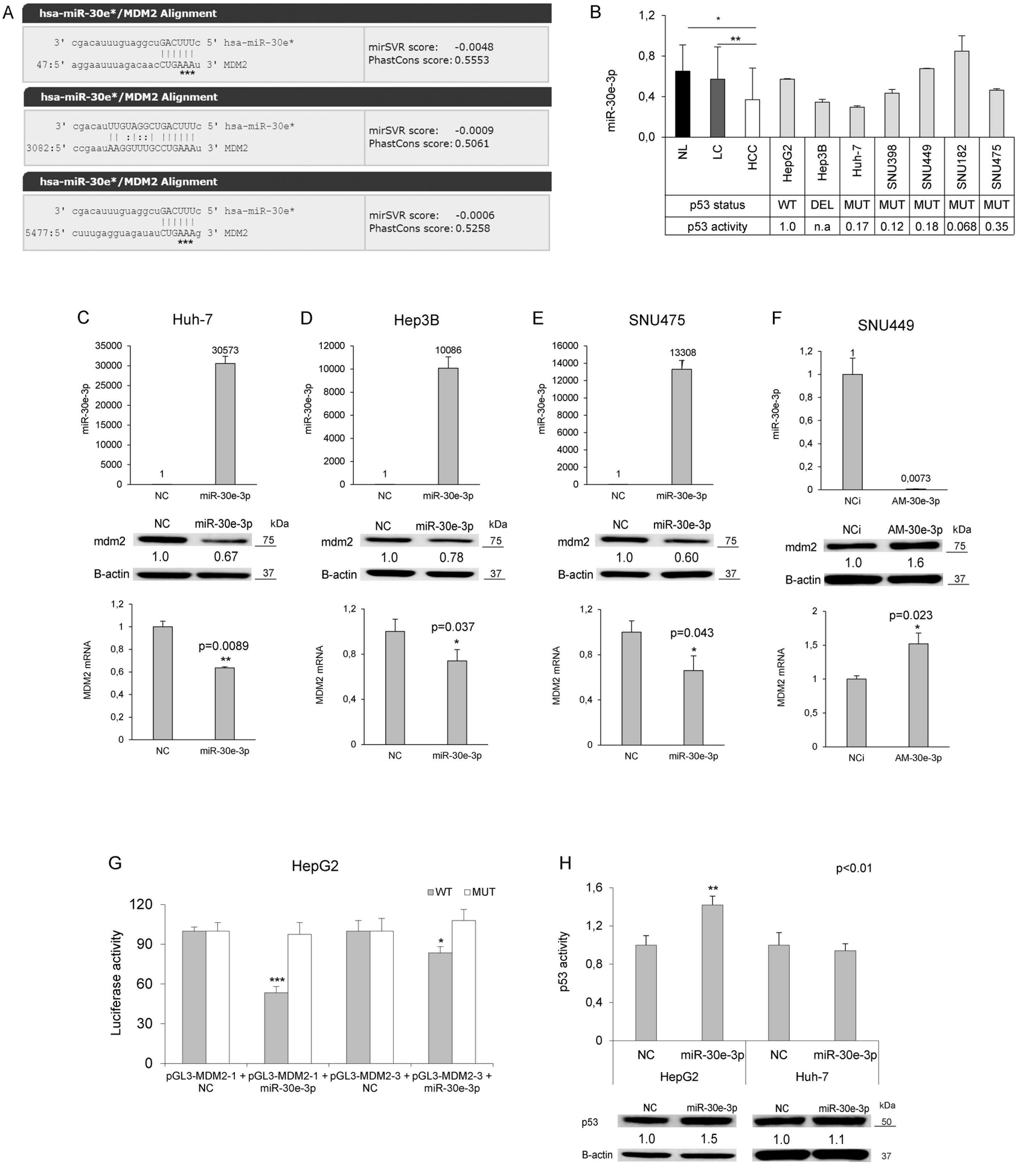
A
hsa-miR-30e*/MDM2 Alignment
3' cgacauuuguaggcuGACUUUc 5' hsa-miR-30e*
47:5' aggaauuuagacaacCUGAAAu 3' MDM2
mirSVR score: -0.0048
PhastCons score: 0.5553
hsa-miR-30e*/MDM2 Alignment
3' cgacauUUGUAGGCUGACUUUc 5' hsa-miR-30e*
3082:5' ccgaauAAGGUUUGCCUGAAAu 3' MDM2
mirSVR score: -0.0009
PhastCons score: 0.5061
hsa-miR-30e*/MDM2 Alignment
3' cgacauuuguaggcuGACUUUc 5' hsa-miR-30e*
5477:5' cuuugagguagauauCUGAAAg 3' MDM2
mirSVR score: -0.0006
PhastCons score: 0.5258
B
miR-30e-3p
NL
LC
HCC
HepG2
Hep3B
Huh-7
SNU398
SNU449
SNU182
SNU475
p53 status
WT
DEL
MUT
MUT
MUT
MUT
MUT
p53 activity
1.0
n.a
0.17
0.12
0.18
0.068
0.35
C
Huh-7
D
Hep3B
E
SNU475
F
SNU449
miR-30e-3p
NC
miR-30e-3p
kDa
mdm2
B-actin
75
37
1.0
0.67
1.0
0.78
1.0
0.60
NCi
AM-30e-3p
1.0
1.6
MDM2 mRNA
p=0.0089
p=0.037
p=0.043
p=0.023
G
HepG2
WT
MUT
Luciferase activity
pGL3-MDM2-1 + NC
pGL3-MDM2-1 + miR-30e-3p
pGL3-MDM2-3 + NC
pGL3-MDM2-3 + miR-30e-3p
H
p<0.01
p53 activity
HepG2
Huh-7
p53
50
1.0
1.5
1.0
1.1

Figure 4

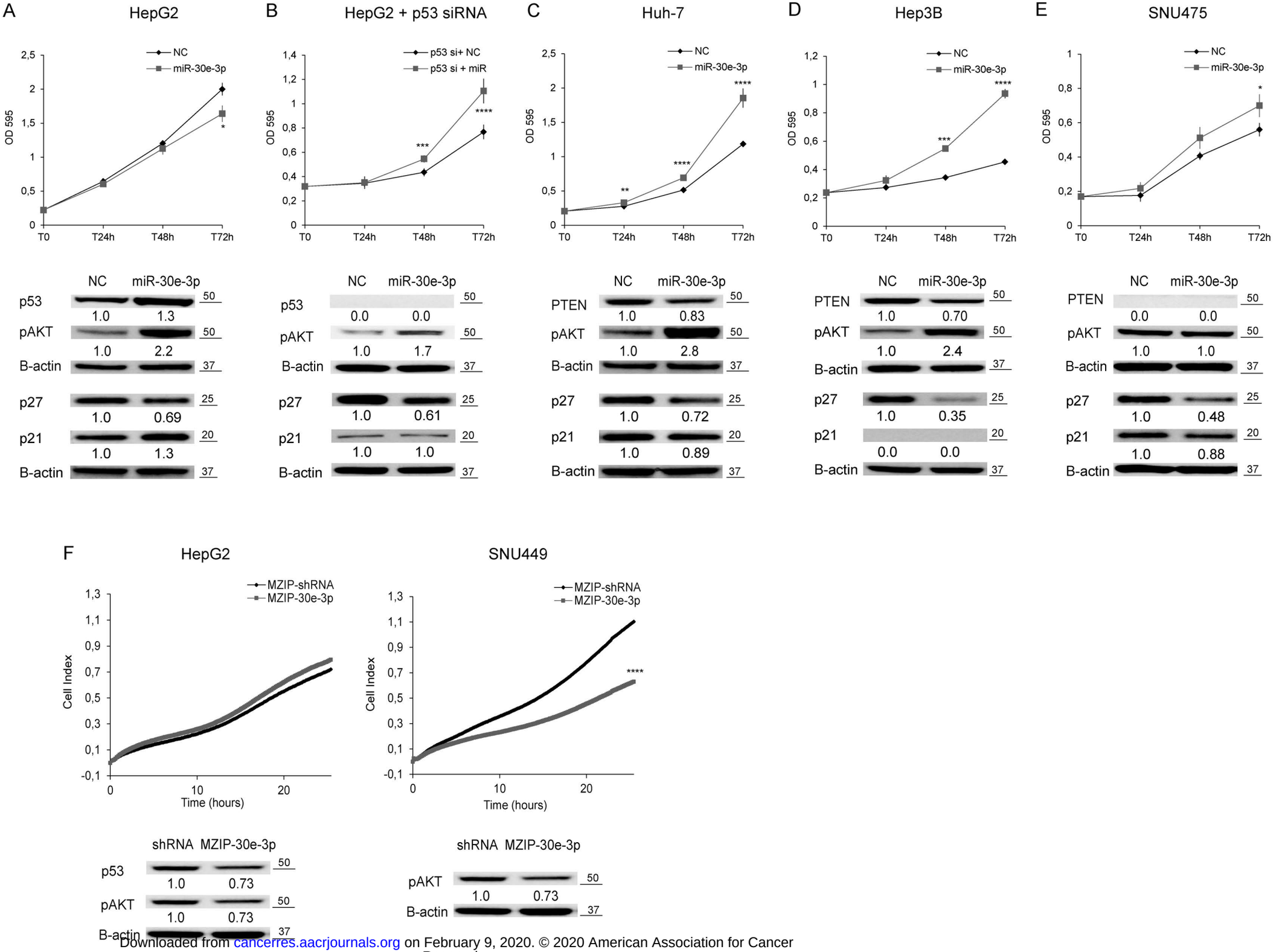

Author Manuscript Published OnlineFirst on February 3, 2020; DOI: 10.1158/0008-5472.CAN-19-0472
Author manuscripts have been peer reviewed and accepted for publication but have not yet been edited.

Figure 5

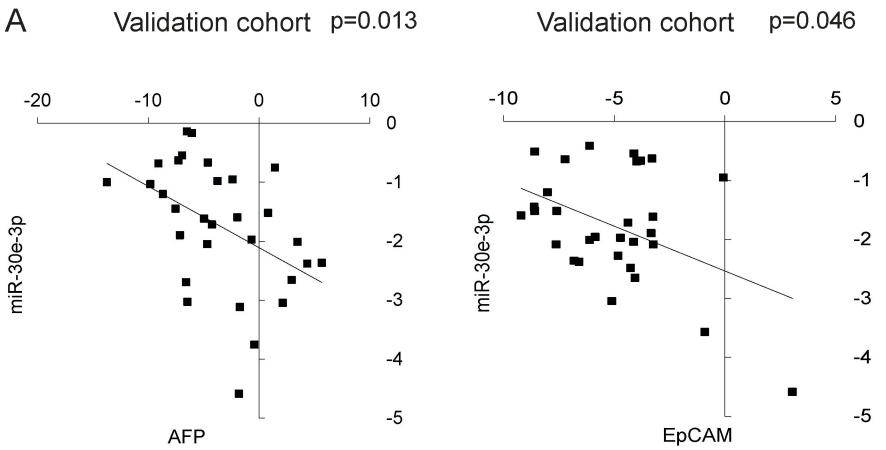

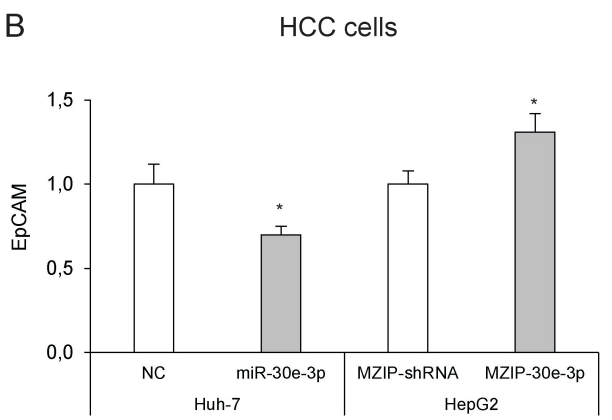

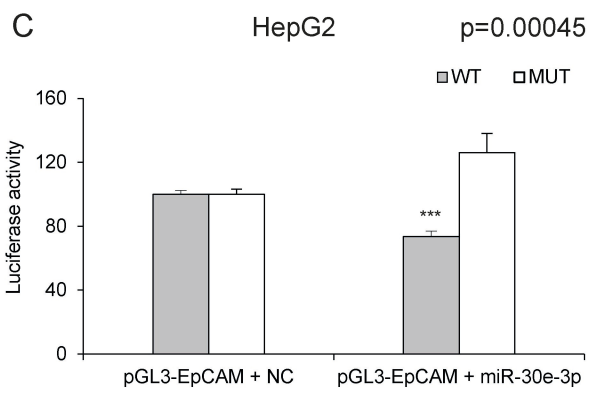

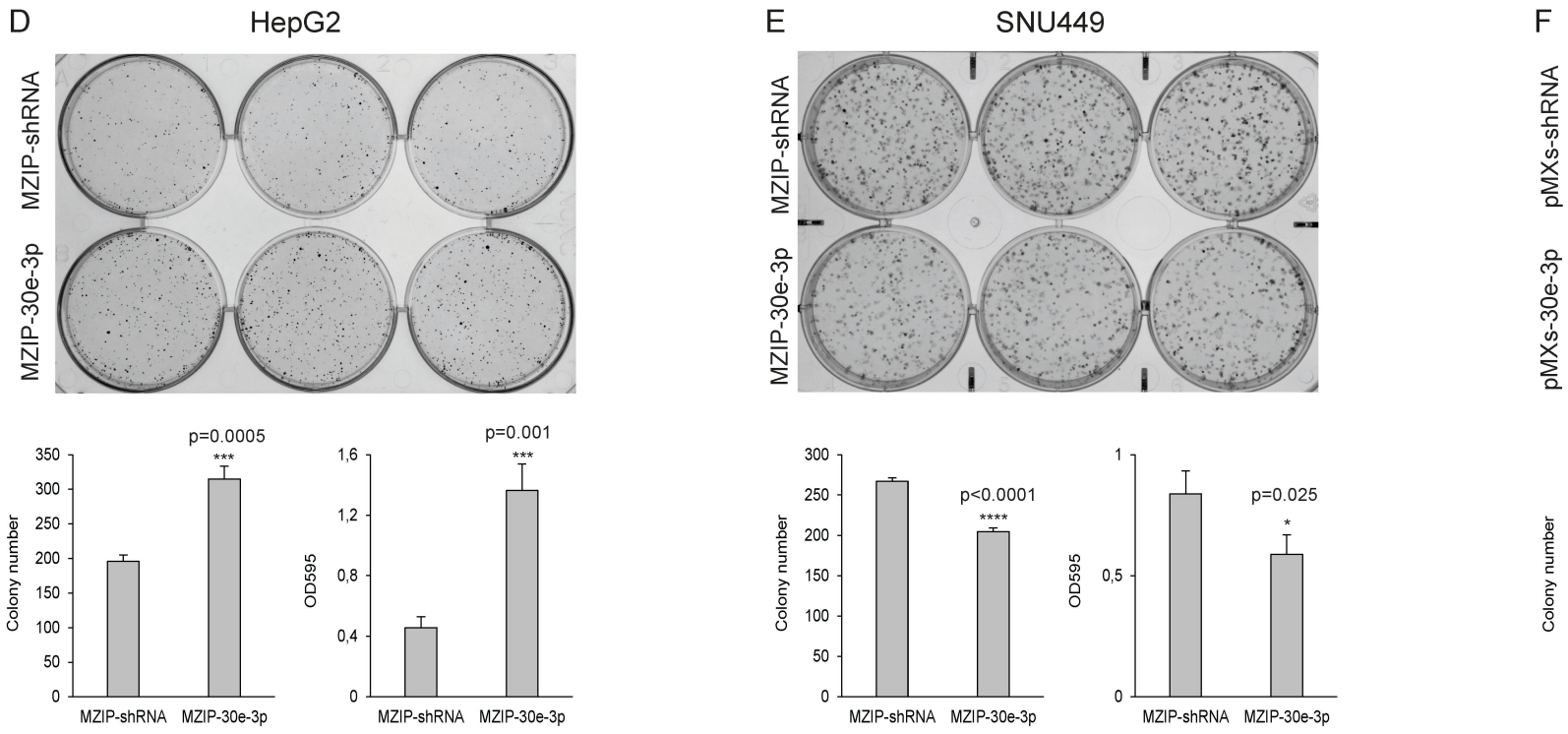

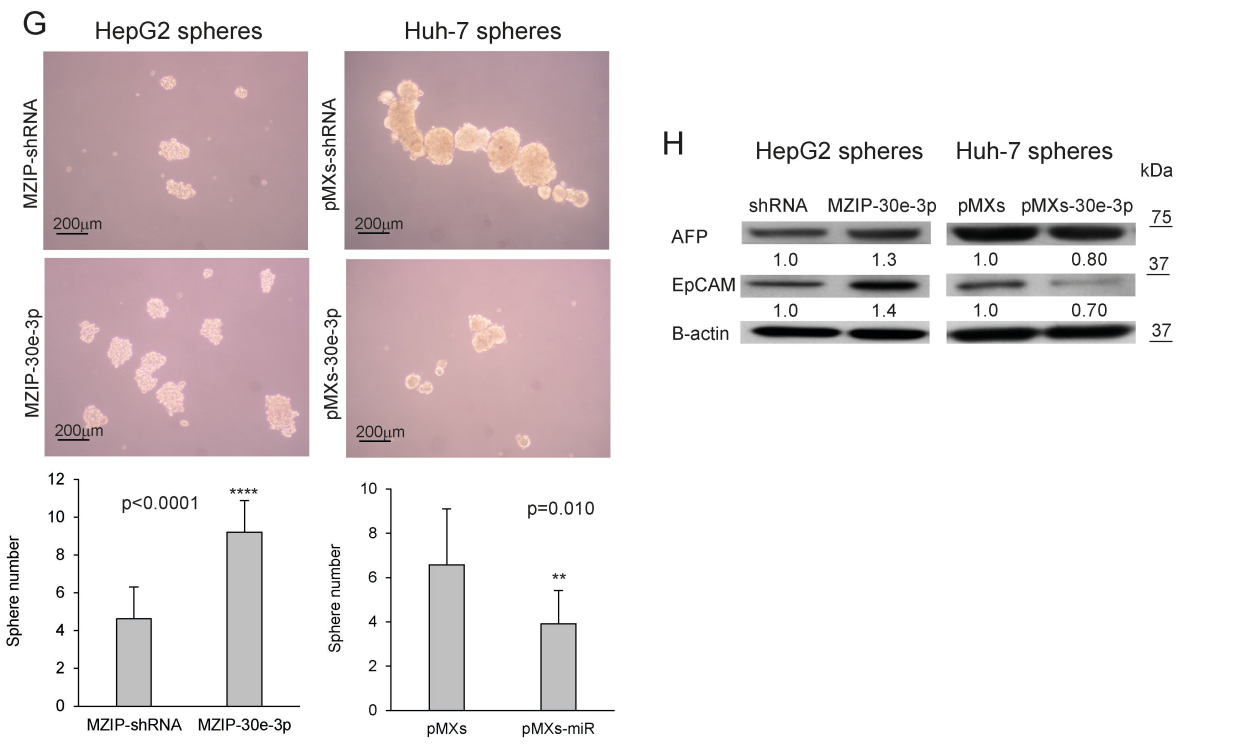

Figure 6

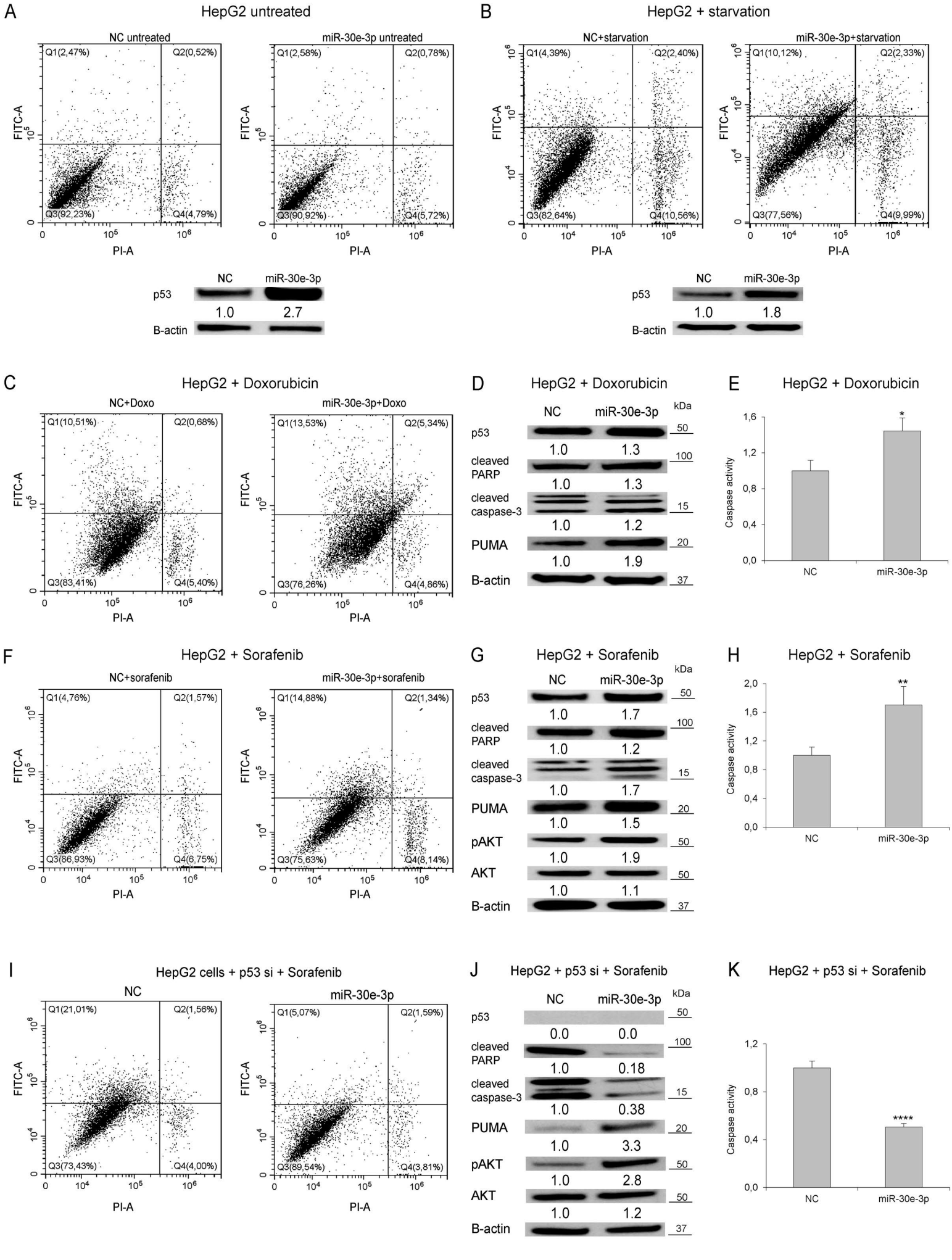
A
HepG2 untreated
NC untreated
Q1(2,47%)
Q2(0,52%)
Q3(92,23%)
Q4(4,79%)
miR-30e-3p untreated
Q1(2,58%)
Q2(0,78%)
Q3(90,92%)
Q4(5,72%)
FITC-A
PI-A
NC
miR-30e-3p
p53
1.0
2.7
B-actin
B
HepG2 + starvation
NC+starvation
Q1(4,39%)
Q2(2,40%)
Q3(82,64%)
Q4(10,56%)
miR-30e-3p+starvation
Q1(10,12%)
Q2(2,33%)
Q3(77,56%)
Q4(9,99%)
p53
1.0
1.8
B-actin
C
HepG2 + Doxorubicin
NC+Doxo
Q1(10,51%)
Q2(0,68%)
Q3(83,41%)
Q4(5,40%)
miR-30e-3p+Doxo
Q1(13,53%)
Q2(5,34%)
Q3(76,26%)
Q4(4,86%)
D
HepG2 + Doxorubicin
kDa
p53
1.0
1.3
50
cleaved PARP
1.0
1.3
100
cleaved caspase-3
1.0
1.2
15
PUMA
1.0
1.9
20
B-actin
37
E
HepG2 + Doxorubicin
Caspase activity
*
NC
miR-30e-3p
F
HepG2 + Sorafenib
NC+sorafenib
Q1(4,76%)
Q2(1,57%)
Q3(86,93%)
Q4(6,75%)
miR-30e-3p+sorafenib
Q1(14,88%)
Q2(1,34%)
Q3(75,63%)
Q4(8,14%)
G
HepG2 + Sorafenib
p53
1.0
1.7
50
cleaved PARP
1.0
1.2
100
cleaved caspase-3
1.0
1.7
15
PUMA
1.0
1.5
20
pAKT
1.0
1.9
50
AKT
1.0
1.1
50
B-actin
37
H
HepG2 + Sorafenib
Caspase activity
**
NC
miR-30e-3p
I
HepG2 cells + p53 si + Sorafenib
NC
Q1(21,01%)
Q2(1,56%)
Q3(73,43%)
Q4(4,00%)
miR-30e-3p
Q1(5,07%)
Q2(1,59%)
Q3(89,54%)
Q4(3,81%)
J
HepG2 + p53 si + Sorafenib
p53
0.0
0.0
50
cleaved PARP
1.0
0.18
100
cleaved caspase-3
1.0
0.38
15
PUMA
1.0
3.3
20
pAKT
1.0
2.8
50
AKT
1.0
1.2
50
B-actin
37
K
HepG2 + p53 si + Sorafenib
Caspase activity
****
NC
miR-30e-3p

Figure 7

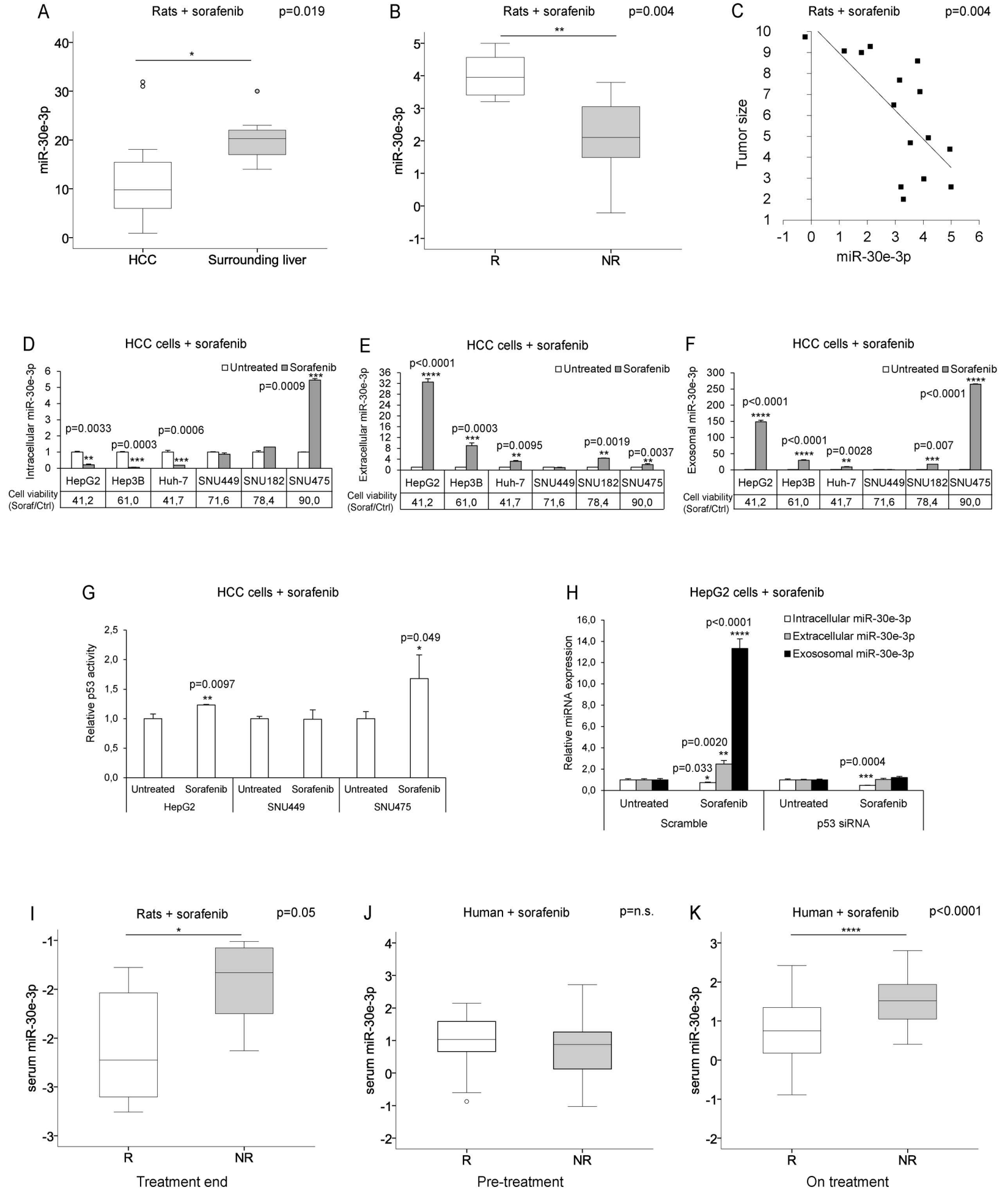
A
Rats + sorafenib
p=0.019
miR-30e-3p
HCC
Surrounding liver
B
Rats + sorafenib
p=0.004
miR-30e-3p
R
NR
C
Rats + sorafenib
p=0.004
Tumor size
miR-30e-3p
D
HCC cells + sorafenib
Untreated
Sorafenib
Intracellular miR-30e-3p
p=0.0033
p=0.0003
p=0.0006
p=0.0009
HepG2
Hep3B
Huh-7
SNU449
SNU182
SNU475
Cell viability (Soraf/Ctrl)
41,2
61,0
41,7
71,6
78,4
90,0
E
HCC cells + sorafenib
Untreated
Sorafenib
Extracellular miR-30e-3p
p<0.0001
p=0.0003
p=0.0095
p=0.0019
p=0.0037
HepG2
Hep3B
Huh-7
SNU449
SNU182
SNU475
Cell viability (Soraf/Ctrl)
41,2
61,0
41,7
71,6
78,4
90,0
F
HCC cells + sorafenib
Untreated
Sorafenib
Exosomal miR-30e-3p
p<0.0001
p<0.0001
p=0.0028
p=0.007
p<0.0001
HepG2
Hep3B
Huh-7
SNU449
SNU182
SNU475
Cell viability (Soraf/Ctrl)
41,2
61,0
41,7
71,6
78,4
90,0
G
HCC cells + sorafenib
Relative p53 activity
p=0.0097
p=0.049
Untreated
Sorafenib
HepG2
SNU449
SNU475
H
HepG2 cells + sorafenib
Intracellular miR-30e-3p
Extracellular miR-30e-3p
Exososomal miR-30e-3p
Relative miRNA expression
p<0.0001
p=0.0020
p=0.033
p=0.0004
Untreated
Sorafenib
Scramble
p53 siRNA
I
Rats + sorafenib
p=0.05
serum miR-30e-3p
R
NR
Treatment end
J
Human + sorafenib
p=n.s.
serum miR-30e-3p
R
NR
Pre-treatment
K
Human + sorafenib
p<0.0001
serum miR-30e-3p
R
NR
On treatment